5. PHYSICAL OCEANOGRAPHY AND ASSOCIATED TASKS DURING MOSAIC LEG 2

Team on board: David Kuhmley[1], Ivan Kuznetsov[1](group leader), Hailong Liu[3], Maria Patricia Mallet[1], Volker Mohrholz[2], Benjamin Rabe[1]

Further collaborators:
Sandra Tippenhauer[1] (not on board)
Rainer Graupner[1] (not on board)
Markus Janout[1] (not on board)
Ilker Fer[4] (not on board)
Arild Sundfjord[5] (not on board)
Celine Heuze[6] (not on board)
Monika Rhein[7] (not on board)
Christian Mertens[7] (not on board)
Yusuke Kawaguchi[8] (not on board)
Ying-Chih Fang[1] (on board Leg 1)
Mario Hoppmann[1] (on board Leg 1)

[1]AWI
[2]IOW
[2]SIO
[3]PRIC
[4]University of Bergen
[5]NPI
[6]University of Gothenburg
[7]University of Bremen
[8]University of Tokyo

Grant-No. AWI_PS122_00

A comprehensive summary of the physical-oceanographic measurements during all 5 cruise legs can be found in Rabe et al., 2022.

Background and Objectives

General physical oceanography of the central Arctic Ocean: brief specifics for leg 2

General background and objectives of the physical oceanography have been described in the expedition booklet, the report by leg 1 and the individual proposals within team OCEAN. Here, we detail only the scientific motivation related to leg 2. The setup and work at sea during leg 2 are described in detail, referring to prior expedition reports only for further detail of the general setup of Ocean City and the Polarstern ice hole.

The drift during leg 2 lead us from the inner basin conditions north of the Laptev Sea into the central Arctic interior, close to the North Pole. The drift crossed the basin and started close to the boundary current region, where water masses are modified by surface forcing and mixing processes involving shelf waters. Further description can be found in the expedition report for PS122/1 and the expedition booklet for PS122. The drift crossed into the northern interior Amundsen Basin. Here, waters have moved away from the dynamically active boundary current, close to the continental shelf, into a more quiescent environment, dominated by diffusive processes in the ocean interior and turbulent mixing only close to the surface (see results section). The whole of the drift described here was in the basin interior, away from intensified currents along the Gakkel and Lomonosov ridges. In addition, seasonally more consolidated ice cover changes the near-surface ocean due to less direct contact between the atmosphere and the ocean. Studying this seasonal variability is part of the main objective of

MOSAiC, in particular, during leg 2, where in-situ observations that require people are not available and only limited autonomous measurements exist.

Auxiliary work & installations

In addition to the planned work described above, it was the responsibility of Team Ocean to deploy various sensors and installations for a number of associated projects in order to augment the observational capacity related to physical oceanography. Due to their variety, we do not provide a scientific background here and refer, instead, to the expedition booklet for PS122. To summarize, we deployed IceBTC60 buoy with 17 thermistors on 60 m cable at 2-5 m spacing, designed for vertical profiling of upper water temperature at the Fort Ridge site; we installed a chain of 3 CTD at the Dark Site SYI (LM site); we deployed 5 T-POP delayed ocean profilers. During leg 2 the deployment procedure of the VMP Upriser turbulence probe in the Ocean City was developed and tested. The use of a small, self-recording CTD for obtaining water column profiles (fishing-rod) and support water sampling (OTE Niskin-style water bottles) in cold conditions was further developed and used for several applications: the lead events and the inter-calibration of buoys at DN sites. Fishing-rod based MSS casts were performed during lead event.

Work at sea

Large hydrohole close to the ship

We regularly operated a CTD/Rosette system with various additional sensors and OTE Niskin bottles (further CTD) as one of the main instruments for measurements of the ocean properties during two days each week. The system was operated through a hydrohole in the ice close to the ship by ship cranes and winches. This ability was also of particular importance with regard to the extensive water sampling program planned for MOSAiC by Teams OCEAN, ECO and BGC, and further enforced by their high demand of sample volume. Basic scheme and additional to normal operations extending of the CTD operation was developed prior to MOSAiC expedition and significantly modified by Leg 1 and further by leg 2. The large hydrohole close to the ship was established early during Leg 1 approximately 8-10 meters away from the ship due to complicated ice conditions in the immediate proximity to the ship. The range for CTD operation on the side of the ship was extended to the hydrohole by using an additional block on the cargo crane. Detailed explanation of the preparation of the hole and combination of cargo crane with main CTD winch for CTD/Rosette deploying was described in cruise report of Leg 1.

Detailed planning of crane operations, including the CTD, shifting heavy loads between the ice and the ship and helicopter operations ensured that no significant delays for CTD, cargo and helicopter operations occurred. In addition, using the cargo crane limited CTD operation to temperatures above -30°C. This necessitated moving the operation in time or even skip a number of CTD casts and further instrument deployments related to water sampling (mainly ECO team). Using the cargo crane increased the total time of CTD casts and being CTD at cold conditions. Overall, using the crane was the only viable option to operate the CTD from the ship during legs 1 and 2. The dimension of the hydrohole was about 3 x 3 m2, sufficient for deploying the CTD and other devices. The edges of the hole were secured with wooden plates for safe operations.

More details of improvement could be found in the ECO part of this report and in the MOSAiC log book. Maintenance of the ice holes both in Ocean City and near the ship took an enormous amount of personnel time. Tests in Ocean City near the beginning of leg 2 showed that a heated tent over the ice hole without operating a submersible pump stirring up the water column under the ice provided enough heat flux to the water to avoid significant formation of new ice. Using a submersible pump, in fact, increased ice formation. The water temperature in the first several meters below the ice is close to the friezing point. By pumping water from

below to ice hole increase loos of heat from water in ice hole that was heated by air inside the tent. The air temperature in the Ocean City tent was about 10°C. After discussion between the BGC, ECO and OCEAN teams a spare Weatherhaven tent was assembled near the ship and installed on top of the hydrohole there. An air heater powered by the ship with a maximum power of 15 kW was placed in the tent. First tests with maximum power showed significant overheating of the tent: on one side this prevented new ice formation, on the other hand produced unwanted melting of ice around the hydrohole. Adjusting the power according to wind and outside air temperature prevented significant melt on the sides of the hydrohole while largely preventing ice formation on the surface of the hole. Replacing the wooden lid that had covered the hydrohole during leg 1 and part of leg 2 by the Weatherhaven tent (PS tent) and heater significantly decreased the amount of time needed for ice hole maintenance or moving the heavy wooden lid by crane. The submersible pump was only used to mitigate ice growth in the hydrohole during CTD cast and nets operations (c.a. 4 hours). The rest of the time the pump was switched off. Moving the tent required 4-6 people before and after use of the hydrohole. For detailed figures see figure 6.1 (ECO team report leg 2) and Figure 5.2.

Fig. 5.1: Left (from Leg 1 report): View from the working deck of the main hydrohole for operation of the main CTD/Rosette and the different nets. Every other day, the hydrohole had to be cleared of newly-grown ice before CTD operation. When no instruments were operated in the hole, it was covered by a wooden lid for isolation and safety reasons (the wooden lid is in the lower central part of the figure). Right: View from upper deck of the hydrohole (1) with tent (2). Ice blocks (3) removed by leg 1 with swiss-cheese technique. (4) cargo crane with block for CTD winch crane (5).

Additional aspects of operation of the ship CTD/Rosette system during Leg 2

Operation procedure of the main CTD during cold conditions (down to -30° C) relative to usual operation temperatures was described in the report of Leg 1 and in supported document of leg 1. Leg 1 reported no single cases in which the sensors were frozen. During Leg 2 we had a situation when sensors of temperature and salinity showed unexpected values near the surface. This could always be resolve by lowering the CTD down to the warmer layers (to about 200 meters) where the temperature was about 0 or +1 °C. In most cases the sensors started to work properly after a few minutes of warming in deeper water. The situation occurred only when sensors were wet prior to deployment, e.g. between casts or when flushing the sensors with salt water prior to the cast. We resolved this issue by flushing the sensors before each deployment with 1:1 mixture of clean salt water (1000 meters depth from previous casts) and bio-ethanol, using syringes and hoses to connect to the CTD pumped inlets.

Summary of the ship-based CTD/Rosette work

The Polarstern CTD/Rosette had been assembled at AWI before the cruise. In addition to the electronic sensors, the rosette had 24 12-liter OTE bottles. A standard SeaBird SBE9plus system was vertically attached to the rosette, and was equipped with double sensors for measuring temperature, conductivity and oxygen. Furthermore sensors for pressure, substance fluorescence (Chl.*a* and CDOM), irradiance, beam transmission and nitrate were attached (Tab. 5.1). The system was additionally equipped with a stand-alone (recording, battery-powered) Underwater Vision Profiler (UVP, see Team ECO chapter 6.2). Finally, an altimeter was mounted to monitor the distance to the seafloor (which started to catch an echo at ~40 m above the bottom). A Rhodamine sensor was installed near the end of leg 2, as described below. The SBE9plus was connected via the 11 mm diameter conducting cable to an SBE11 surface unit.

Deep CTD casts were done to ~10 m above the seafloor. The actual water depth matched the calculated and sound-speed corrected EK60 water depth with an uncertainty of 2 m.

Leg 2 CTD cast schedules were established during leg 1 and continued by leg 2. Ship-based CTD casts were done regularly up to four times a week, and usually on Thursday and Friday (and occasionally on Saturday). The water budget and sampling sequences of different parameters was discussed among the different teams before each cast. During Leg 2, as well as leg 1 Team BGC only requested a minor amount of water samples from the ship-based CTD/Rosette, while the majority of the water demand came from Team ECO. Team OCEAN required water samples for CFC/SF6 and salinity calibrations during deep (>1000 m) casts, as well as water samples for CFC/SF6, helium and tritium from shallow casts (< 500 m). Based on the discussion, Team ECO prepared a draft water budget plan for the ship-based water samplings. It was Team OCEAN's responsibility to prepare and operate the CTD/Rosette system. Maintenance of CTD hole was done by joint efforts of teams ECO, OCEAN and BGC. Deployment of the CTD were done also by joint efforts of teams ECO, OCEAN and BGC. At least 4 persons from the science side were simultaneously involved in CTD deployment.

After installing the tent, net deployments were mainly conducted on Tuesday and Wednesday. On Thursday, a shallow CTD cast was usually conducted first, followed by a short net deployment or other crane operations to shift heavy equipment on demand. The deep cast usually started before 11:30, when the gangway was lifted up for 1 ½ h during lunch. The cast was continued over lunch so that the cast could be carried out from the winch control room on the ship while the CTD was in the water. A full depth cast to 4400 m took about 4 hours, so that the CTD could be recovered after 13:00. Overall, 32 CTDs were deployed from Polarstern, 10 of which were deep casts (see Tab. 5.7). Once water sampling was finished, the raw CTD data was pre-processed following standard procedures (see CTD/rosette data processing). The data was provided to the MCS, and quicklooks were made available (see Preliminary Results section).

Tab. 5.1: Sensor configuration of the Polarstern CTD/Rosette system. Sn = serial number.

	Temperature sensor	**Conductivity sensor**	**Oxygen sensor**	**Pressure sensor**	
Primary	SBE3 sn #1338	SBE4 sn #3173	SBE43 sn #1834	sn #0321	
Secondary	SBE3 sn #1374	SBE4 sn #3590	SBE43 sn #0467	-	-
Altimeter	**Transmissometer**	**Nitrate sensor**	**Chl-a Fluorometer**	**PAR/Irradiance sensor**	**CDOM Fluorometer**

Sn 47768	WET Labs C-Star sn #1198	Satlantics SUNA sn #0732	WET Labs ECO-AFL/FL sn #725	Biospherical/ Licor sn #70257	WET Labs ECO CDOM sn #4531

In addition to the sensors listed in Table 5.1, we installed a c fluorescence sensor, a Turner Cyclops fluorometer for Rhodamine. The sensor with serial # 216k00137 was calibrated on the Polarstern CTD/Rosette using Rhodamine solutions of known concentration, prepared with standard Rhodamine tabs, a set of scales, several beakers and burettes with calibrated volume, on-board. The result of this calibration is shown in Table 5.X.

Near the end of leg 2, we installed the, yet uncalibrated, sensor #216K00138 on the Polarstern CTD/Rosette and switched the calibrated one to the Ocean City CTD/Rosette.

Vessel mounted current profiler of RV Polarstern

Polarstern is equipped with a shipboard Acoustic Doppler Current Profiler (SADCP) to monitor underway ocean currents. The Ocean Surveyor (frequency 150kHz, beam angle 30deg), manufactured by RD-Instruments, was mounted downward looking behind a window in the ship's hull, flooded with water. The data output of the ADCP was merged online with the corresponding navigation data and stored on the hard disc using the program VMDAS. Pitch, roll and heading data are converted from NMEA. Current data were collected in beam coordinates to apply all corrections during post processing. The VMADCP was operated continuously during leg 2 of MOSAiC.

Leg 2 used the configuration of the SADCP by leg 1 from 28 October.

Processing of the VMADCP data on board was carried out using the Matlab® ADCP toolbox of IOW. The resulting profiles are 300s averages of the single ping profiles. The heading bias of the instrument and the magnetic deviation were applied during post processing.

Due to the low abundance of appropriate scatters the performance of the device was limited. Reliable current data were gathered between 25m and 250m water depth.

Final processing of MOSAiC SADCP data will be carried out with the Matlab® ADCP toolbox by GEOMAR Helmholtz Centre for Ocean Research Kiel with minor changes implemented at AWI

Ocean City

The preparation and installation of Ocean City was carried out during leg 1. The installation procedure and setup of the main instruments were detailed in the corresponding expedition report. During Leg 2 there were no significant cracks and leads in the MOSAiC CO. Thus, no reallocation of Ocean City similar to leg 1 was necessary. Ocean City was secured by 4 straps anchored to the ice to resist to strong winds. A PAR sensor was installed on a telescope stick, fixed between tent straps, and the sensor was connected to the deck unit of the OC CTD (the electronic setup had been prepared by leg 1). The KC Denmark winch, which was not used during leg 1, was tested and used for LISST deployment during the second part of leg 2 (see LISST deployment). We had one "black out" power failure during leg 2, affecting the whole CO for a several hours. During that time the tent was not heated and the temperature inside the tent dropped to about -8 °C. As all sensors, except the pump duct of the CTD, were dry there was no damage to the equipment in the tent. The mixture of 1:1 seawater and ethanol avoided damage to the CTD, that had previously been stored dry. This was changed due to potential issues with dry residue on the conductivity sensors. During several storms with winds gust of up to 25 m/s and low temperature (wind-chill temperature lower down to -60° C) the Ocean City tent showed good performance. The temperature in the tent was rather stable in time, varying spatially within the tent between 0 °C (near some of the corners) and 15 °C (near main heating area, close to the CTD). Work in the tent was possible during the entirety of leg 2 with few exceptions due to low visibility (bear guarding was not possible due to safety

regulations). Two “24 hour“ stations took place at Ocean City. Each set included two CTD casts before and after a series of MSS casts (24 hours). MSS casts were performed by one person from team OCEAN in the tent and one outside of the tent as a bear guard. The ice hole in the OC tent was equipped with a rope-ladder to allow a safe escape from the hole in case a person fell into the ice hole. However, no incidents of this kind occurred throughout leg 2. Regular, daily work in the OC tent was performed by at least two persons inside the tent and one bear guard outside. OC bear guarding was carried out by team OCEAN most Mondays, Tuesdays, Wednesdays and Saturdays. Bear guards from the Logistic team covered most Thursdays and Fridays, when three members of the OCEAN team were busy with CTD casts on-board Polarstern. On Sundays one of the two weekly LISST casts were carried out and usually supported by a bear guard from the Logistics team. In addition, the Logistics team was in charge of bear guarding OC during several storms, when visibility and cold conditions required professional support, and partly during the weeks before the transition between legs 2 and 3.

CTD/Rosette casts in Ocean City

The CTD/Rosette system in Ocean City is essentially a smaller version of the ship-based CTD/Rosette. It was assembled and tested at AWI before the cruise as well as during Leg 1. The rosette has 12 5-liter OTE bottles. In the lower part of the frame, a standard SeaBird9plus system is mounted horizontally and equipped with duplicate sensors to measure temperature, conductivetyasnd oxygen. Furhtermore, sensors for pressure, fluorescence (Chl.*a* and CDOM), irradiance, beam transmission, nitrate, and methane concentration/gas temperature are attached (see Tab. 5.2). A rhodamine sensor was installed during leg 2. The SBE9plus was connected via a Rochester (type A210124) 3.12 mm diameter conducting cable to an SBE11 surface unit. The custom-built winch can support safe ascending/descending speeds of ~0.2–0.5 m s^{-1}, and has a cable length of 1500 m. A typical 1000-m profile normally takes about ~3 hours. Overall, 30 CTD deployments were done in Ocean City. Among these deployments, water samples were taken for Teams BGC and ECO. Water samples were also collected occasionally for salinity calibration. After test sampling during leg 1 samples for CFC/Helium/Tritium were not taken from OC during leg 2, sampling for these parameters were done with PS CTD. Similar to the ship-based CTD/Rosette data, pre-processed data were copied to the MCS, and quicklooks were prepared (see Preliminary Results).

Tab. 5.2: Sensor configuration of the Ocean City CTD.

	Temperature sensor	**Conductivity sensor**	**Oxygen sensor**	**Pressure sensor**	
Primary	SBE3 sn #4918	SBE4 sn #3549	SBE43 sn #1605	sn #0935	
Secondary	SBE3 sn #5110	SBE4 sn #3810	SBE43 sn #0743	-	-
Altimeter	**Transmissometer**	**Nitrate sensor**	**Chl-a Fluorometer**	**PAR/Irradiance sensor**	**Methane sensor**
N/A	WET Labs C-Star sn #1220	Satlantics SUNA sn #1318	WET Labs ECO-AFL/FL sn #1346	Biospherical/Licor sn #70241	Franatech METS sn #1917

The Turner Cyclops fluorometer for Rhodamine # 216k00137 was installed on the Ocean City CTD/Rosette near the end of leg 2; however, there were issues with using the sensor on a custom-made split cable, also running the Franatech methane sensor (data and power) and the SUNA (power only). These issues, related to the methane sensor needing two channels for output (methane concentration and temperature), could not be resolved before handover.

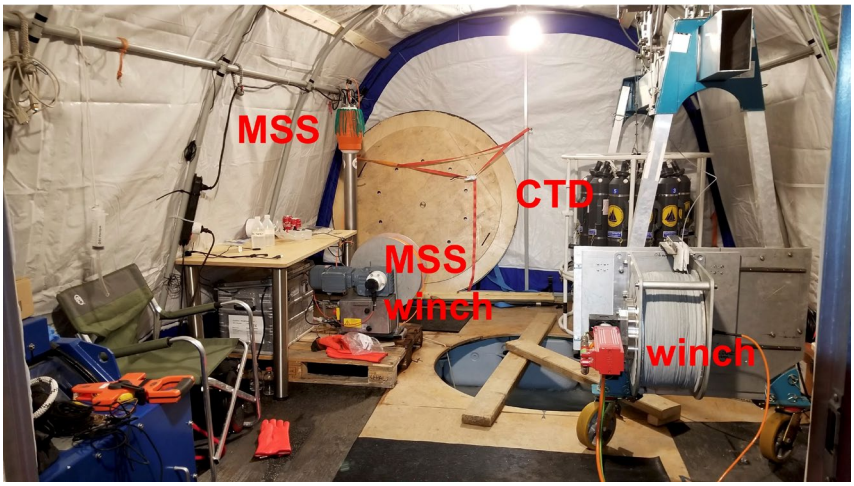

Fig. 5.2: Pictures from Leg 1 report. Interior view of the Ocean City 2.0 Weatherhaven tent. The hydrohole is below the circle-shaped hole next to the MSS winch, and was usually covered by a small bridge for easy passage.

CTD/rosette data processing

Data collected from CTD operation were pre-processed using ManageCTD matlab software and SeaBird data processing software. However, most of the plots in this report that contain CTD/rosette data were produced using only the SeaBird data processing software. Different routines were used accordingly before 1 dB bin-averaged ASCII output .cnv file and .btl (bottle) file are produced. These routines are DATCNV, WILDEDIT, BOTTLE SUMMARY, SPLIT, TRANSLATE, CELL THERMAL MASS, LOOP EDIT, and BIN AVERAGE. Only downcast profiles were used to produce ASCII .cnv files, which contain both original and bin-averaged profiles. Team OCEAN submitted raw data to the MCS system and pre-processed files to quicklooks. Team OCEAN provides figures for various depth range (0-100, 0-350, 0-1000, 0-full depth) and bottle files to quicklooks for an overview of CTD operations.

Microstructure profiling at Ocean City

The turbulence measurements at Ocean City were performed with microstructure-turbulence profilers MSS 90-S (Serial numbers 46, 55, and 75). This profiler is an instrument for simultaneous measurement of microstructure and precision measurements of physical parameters in marine waters. The MSS profilers were equipped with 2 velocity microstructure shear sensors (for turbulence measurements), a microstructure temperature sensor, and standard CTD sensors for precision measurements, and a vibration control sensor. Some of the profilers have additional Oxygen, turbidity or Chlorophyll-a sensors. The particular configuration is given in the following table.

Table 5.3: Sensor configuration of the used MSS profilers

MSS profiler	***S/N***	**46**	**55**	**75**
	Owner	NPI	IOW	AWI
	Sampling rate	1024Hz	1024Hz	512Hz
Sensors	***Pressure***	PA7-50 (500m)	PA7-100 (1000m) PA7-25 (250m)	PA7-100 (1000m)
	Shear 1	PNS 53	PNS 18	PNS 6046
	Shear 2	PNS 54	PNS 19	PNS 6182
	Temperature (PT100)	-2…36°C	-2…36°C	-2…36°C

	Temperature (NTC)	FP07	FP07	FP07
	Conductivity	0…70mS/cm	0…70mS/cm	0…70mS/cm
	Micro conductivity	0…70mS/cm	-	-
	Tilt	ADXL 203	ADXL 203	ADXL 203
	Acceleration	-1…1m/s²	-1…1m/s²	-1…1m/s²
	Oxygen optode	-	SST-DO	SST-DO
	Turbidity	-	SST-Turb	-
	Chlorophyll-a	-	-	Cyclops 7

All sensors are mounted at the measurement head of the profiler, the microstructure ones being placed about 150 mm in front of the CTD sensors. The sampling rate for all sensors depended on the particular probe. During each station a set of 2 to 11 subsequent profiles was gathered. The profile to profile interval ranges from 25 to 35 min. Usually, the observations cover the upper ocean layer between 1.5m and 400m depth. The maximum depth depends on the actual drift speed and varied from 330m to 425m, for high and low drift speed, respectively. The profiler was balanced with negative buoyancy, which gave it a sinking velocity of about 0.6 m/s. It was operated with an electrical winch from the side of the ice hole. Disturbing effects caused by cable tension (vibrations) and the ice drift were excluded by a slack in the cable. After each deployment the sensors were flushed with pure water to prevent fouling. The dissipation rate of turbulent kinetic energy was calculated by fitting the shear spectrum to the theoretical Nasmyth spectrum in a variable wave number range from 2 to a maximum of 15 cycles per meter (cpm). The low wave number cut off at 2 cpm is meant to eliminate contributions from low frequency tumbling motions of the profiler. During leg 2 more than 680 MSS profiles were obtained. The majority of the profiles were taken with MSS46.

A major technical problem during the deployment of MSS75 was a low frequency (0.5Hz) interfering signal on most of the sensor channels. All trials to fix the problem, including the replacement of an electronic board, were not successful. Thus, the MSS75 was not used for usual operation.

In the beginning of leg 2 the NTC temperature sensor of MSS46 produced a cutoff for temperatures below -0.285°C. Most probably this was caused by a sensor output that exceeded the range of the A/D converter of the probe. The NTC sensor was replaced on 17th December 2019. That fixed the issue. However, all measurements taken with this probe during leg 1 of MOSAiC are affected by this issue.

To cover also biological parameters the MSS46 was replaced by the MSS55 on 2nd March 2020 before the beginning of the spring bloom.

For data quality checks of both profilers, MSS46 and MSS55, comparison measurements with the ocean city CTD were performed (Fig. 5.4). The particular profiler was mounted in the CTD frame and lowered together with the CTD down to 200m depth. After post processing and final calibration of the CTD sensors, the MSS sensors will be calibrated with the validated CTD data.

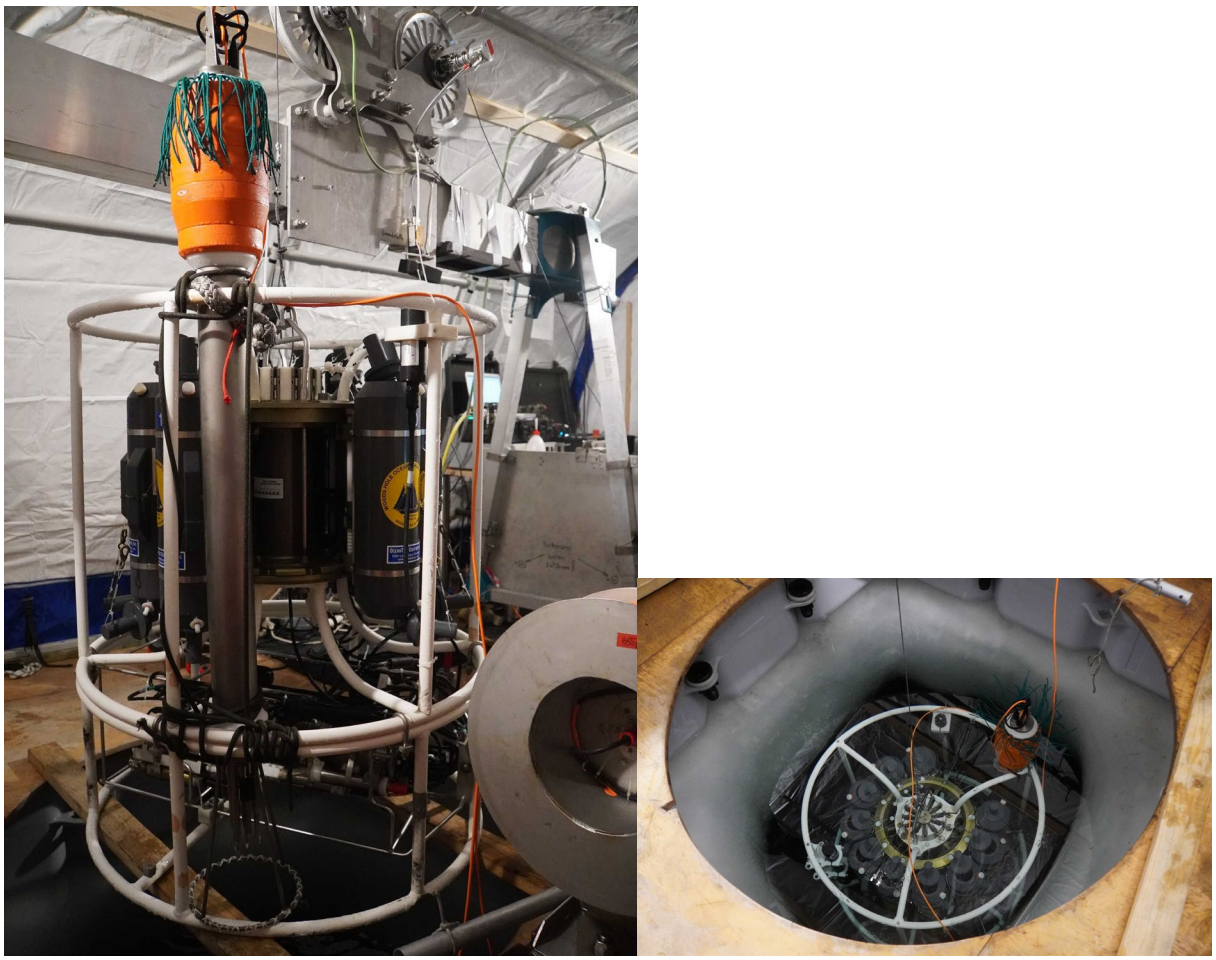

Figure 5.3: Ocean City CTD with mounted MSS profiler for comparison measurements

Current profiler at Ocean City ice hole

To gather concurrent data of currents and turbulence in the mixed layer, a 300kHz ADCP was mounted temporarily in the Ocean City ice hole (fig. 5.5). The device was mounted in a stainless steel frame that kept the heading of the ADCP fixed relative to the heading of the floe. The ADCP gathered reliable data in the upper 50m. It was operated as much as possible, nearly continuously. However, during deployments of the CTD and the LISST profiler the ADCP was removed from the ice hole. Further gaps in the time series were caused by power supply failures and changing of the memory cards once a week.

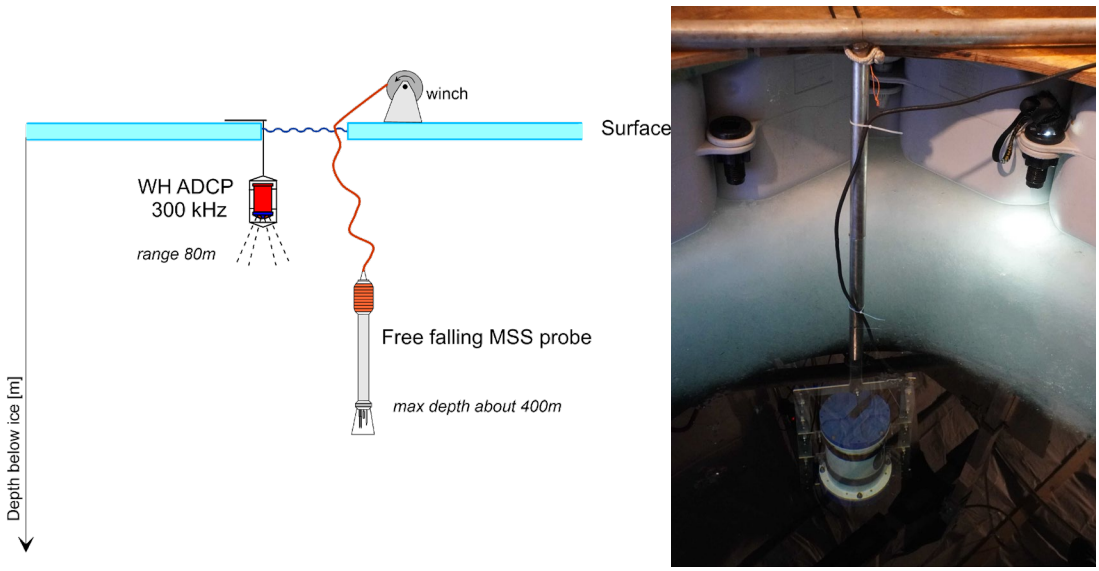

Figure 5.4: Sketch of concurrent measurements with MSS profiler and ADCP in Ocean City ice hole (left), downward looking ADCP (right).

Microstructure profiling with VMP-upriser

VMP-upriser for MOSAiC to allow observation of the under-ice boundary layer, within a few meters from the underside of the ice. The MSS does not provide reliable measurements there due to initial adjustment at the beginning of every downward profile. Knowing turbulence in that part of the water column would be extremely useful, for obvious reasons. Ocean City is the most common location for any turbulence profiling, leads are an option for occasional turbulence profiling from the edge or a nearby ice hole. The original plan was to have Ocean City in an area of fairly level ice, to avoid disturbance of the upper mixed-layer expected close to the ship. For reasons of logistics / ice conditions Ocean City ended up in area of partially ridged ice -- the ridging and subsequent move of OC during leg 1 further added to that, so that OC is now located about 30m either way between ridges, one with a keel of down to 9 m (see ROV survey logbook entry "When Haary met Sally"). There is variable drift of the floe, sometimes >0.5 kn during high winds (e.g. just now). For a VMP profile of 50-100 m we'd expect a significant shift in the VMP location during the upraise (>25 m), relative to the OC ice hole. For low drift, 0.1 kn, it's still 10 m. There is no way to precisely locate the VMP just before it hits the underside of the ice (i.e. if it was close to a ridge or not). The drift direction and speed of OC can be deduced from the ship's navigational record. Test operation during leg 2 (recently) tied up significant personnel, transport to/from OC (could be optimized / storage in tent optimized), three people to run the instrument in the tent, plus BG outside. It's relatively hard physical labor. For comparison, it takes min. 1 person to run the MSS in the tent (although it's usually done with 2 people), plus BG outside.

VMP-u assembling and preliminary testing have been done in the wetlab. During assembling and preparation, it turns out that winch for the rope is broken (some plastic details that hold a rope). It was stored in one of the container right at the end, so it take some time to dig it out. Rope winch itself is mounted to the pallet and rather bulky for transportation between ship and OC (if it is assembled it would be need to involve crane to put it on the ice and sledge). To save our time and space at OC (and to avoid attempt to push it throw OC door or de/re-assembling it in OC) we used only rope and barrel with hand winch. Assembling of VMP-u in OC is problematic (due to space issue (there are big chance just to brake instrument or sensors) and limiting in time work at OC (assembling in OC would need 3 persons including one BG and cutting for a day our measurement program) . We did not attach sensor to the VMP at the first deployment (at the ship), while it was high risk to destroy it during first test

cast. It was done in the OC after test first casts when we were established cast procedure. Programs to communicate with instrument were installed on semi rugged laptop with RS-232 port. While VMP-u was not found by communication program using our connectors (usb-rs). To transport VMP-u to OC MSS wooden box was used. In total we bring to OC : VMP-u with flotation in MSS box, tail that was assembled in OC, details of Weight-Release System with cable drum, additional ropes and carbines with rollers for attaching it to the top of the OC tent for cable and rope passing. Last one we needed while lowering, while lowering over the edge of tent hole and ice edge is not practical and would destroy and tent and cable with rope. Everything was packed in one pulka and on one Nansen sledge +skidoo. In the deployment were involved 3 people from Ocean and one logistic BG. We used one morning slot. First two casts were done without installed sensors. Than sensors (S1 -> M1144, S2 -> M555, C1 -> c165, T1 -> T1127) were attached and two more casts were done, in additional two more casts with MSS were done for comparison. Length of VMP-u is more than diameter of OC hole, that means one need to grab it the water to avoid destroying of unprotected sensors. Using VMP-u with weight in vertical position has high risk to destroy sensors during pulling it under the ice. One more person for caring VMP-u into and out of the water, and lifting by hands of weight-release system with cable. To avoid seizing of VMP-u in CTD hole during take out after last cast additional weight was send on the rope, so weight bring tail of instrument down. In such a way VMP-u could be raise vertically in the middle of the hole. One more person is needed for caring of winch with rope attached to VMP-u. After casts VMP sensors were carefully dried (to avoid destroying because of freezing during transport back) and VMP moved back to the ship. After deployment data were downloaded from VMP-u. After attaching of sensors, setup.cfg on VMP itself was not changed. For post processing proper setup.cfg should be used. Second deployment of the VMP-u was performed during legs 2 and 3 exchange. 3 more profiles were done with old setup.cfg. After second deployment setup.cfg was exchange in VMP-u instrument internal memory. In such a way, data from next casts could be post processed in more simple way. In total 5 profiles with sensors were done (two profiles - PS122/2_25-106 and 3 profiles - PS122/3_29-84).

Figure 5.5: VMP-u assembling and dry test at the WetLab.

Figure 5.6: VMP-u deployment at OC.

Laser In-situ Scatter Transmission meter (LISST)

In addition to the standard CTD and MSS measurements, a Laser In-situ Scatter Transmission meter (hereafter referred to as LISST) was used in order to measure underwater distribution of particle sizes. The ultimate goal of this project is to estimate the export and sequestration of particles beneath the sea ice and consequently impacts on the sensitive ecosystems over the central Arctic as introduced in the cruise report of Leg1. The task of Leg2 is to extend the observation through winter season and contribute to the completeness of an annual cycle. Measurements from this instrument were taken within the framework of a project of the Polar Research Institute of China (PRIC) in order to collect time series of particle sizes in the upper 500–1000 m of the ocean throughout the entire MOSAiC drift.

The LISST was deployed in OC twice a week and down to 500–1000 m. It requires two team member of OCEAN and ECO teams (approximately 4 hours in the Ocean City tent one cast), and 2 bear guards each cast in two shifts. Bear guarding was secured by members of OCEAN team during Wednesdays and logistic team during Sundays.

Deployment in Ocean City before Jan 19 during Leg 2, the LISST-Deep instrument was deployed together with Sea-Bird Electronics 911plus CTD interfaced with a General Oceanics rosette with twelve 5-litre bottles, in the same manner as Leg1 deployment which is described in Section 6.5 of Leg1 cruise report. Due to the concern that the cable for CTD rosette winch may not sustain the added weight of LISST-Deep instrument in following Legs, we have switched to deploy LISST-DEEP with Seacat (SBE19) mobile CTD attached using a separate blue winch from KC Denmark Research Equipment from Jan 19 2020. As shown in Fig.5.7a the cable in blue winch is put up through the stand which is still connected with winch control box (Fig.5.7d) for depth reading. The assembly of SBE19 mobile CTD and LISST instrument (Fig.5.7b) is hung to the end of cable by the connector (Fig.5.7c). We estimate the profiling

speed based on change of depth readings over time and control the speed in range of 0.2-0.5 m/s. All the settings of LISST instrument follow Leg1 setup.

In total, 13 LISST profiles were obtained in Ocean City from December 16 2019 to February 24 2020 with depth range from 500-1000m during the MOSAiC Leg2 expedition (Fig.5.7, Table 1). We had planned to perform the observations twice a week. However, several scheduled deployments were canceled because of unexpected events such as severe weather condition. Although limited in number, these are the first LISST profiles ever acquired over the central Arctic Ocean beneath sea ice through winter.

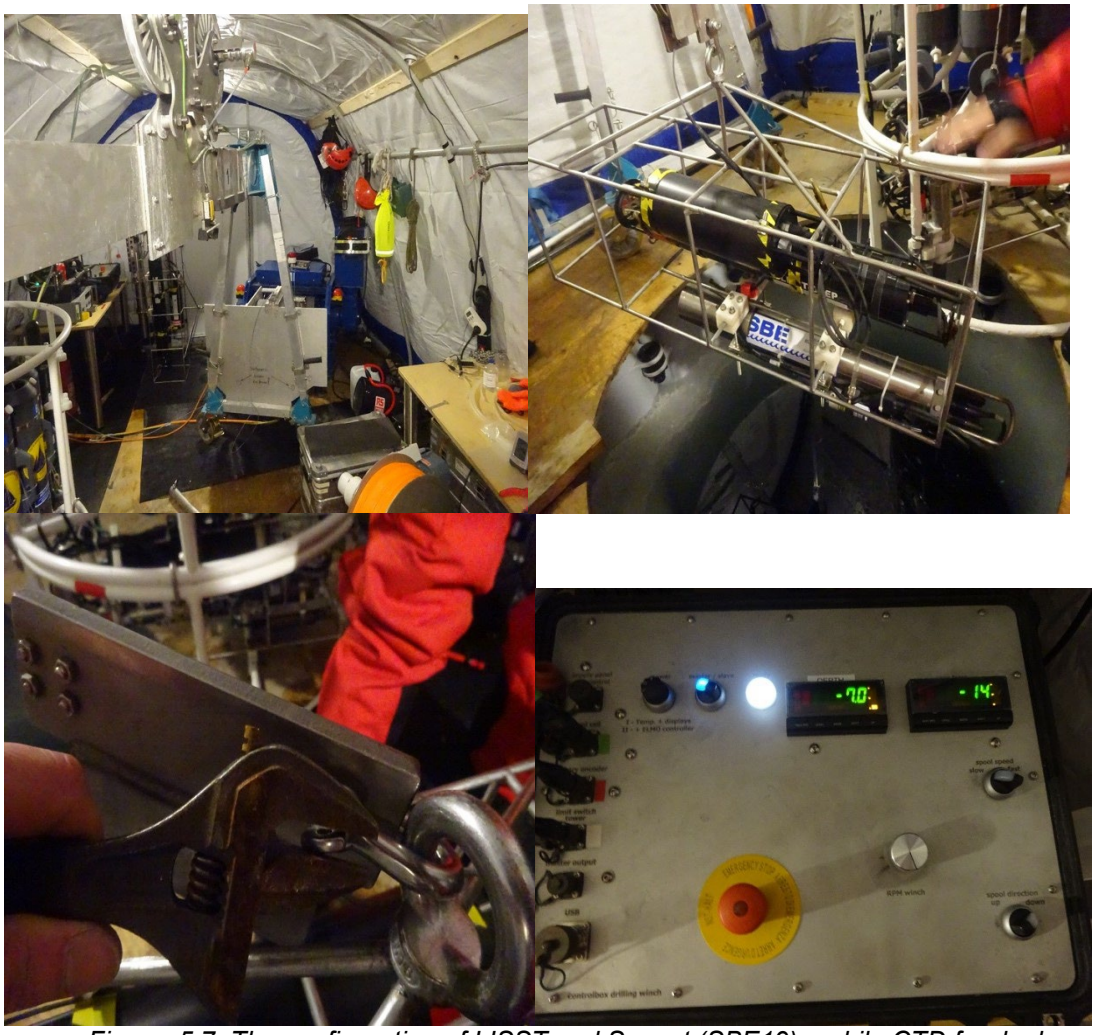

Figure. 5.7. The configuration of LISST and Seacat (SBE19) mobile CTD for deployment

Operation of a small CTD at different locations on the ice floe

We made use of a small type of unpumped CTD, the SST 48M by Sea&Sun Technologies (Germany), to measure temperature, conductivetyand pressure in the upper water column at different locations in and around the CO and different sites in the DN. This is advantageous for obtaining high-quality CTD profiles at remote locations without external power or a heated environment. The SST CTD packages were used in two ways:

- To obtain vertical profiles, we mounted buoyancy (foam rings) on the CTD package and attached it to a line on a fishing rod. We used a small shackle to connect the CTD to the fishing line “whirl” (turning) connector and put a medium-sized cable-tie (disposable) around both the CTD connector and the fishing-line connector to secure the connection further. We obtained a downcast profile by reeling out the line carefully

using the brake. The clutch was always in gear, never in neutral, during reeling out, to avoid sudden...? The rod had a motor winch to reel in the line after each profile.

- We used Niskin-style bottles with a volume of 5 l on an about 5 mm rope to obtain water samples down to 50 m depth. The bottle was triggered with a messenger weight from the ECO team (Multinet messengers). To determine the accurate depth, temperature and salinity of water bottle samples we attached the SST CTD about 1 m below the water bottle, followed by a terminal weight (2 large shackles). This ensured that the bottle was upright on the rope to aid closing triggered by the messenger.

During both modes of operation, ambient temperatures in the field presented a big challenge:

before placing the package into the water care had to be taken to warm the sensors to avoid immediate freezing of seawater inside the sensors. Likewise, the sensors had to be warmed immediately after removing the package from the water. We solved the issue by either placing the sensor in a warm, insulated box before and after deployment, or by using ethanol on the sensors if time was short in between deployments. Nevertheless, we observed unrealistic temperature and salinity values in the upper few meters of several casts, likely due to sensor adjustment.

The insulated box was either a half-height Zarges box, warmed by hot-water bottles or hand warmers; or a large styrofoam box that fit the Niskin-style bottles, likewise heated by hot-water bottles.

We primarily used the SST CTD package with serial #1495.

Both SST CTD packages (serial number #1495 and 1459) were attached to the Polarstern CTD/Rosette during … and ... for later cross-calibration → dship events in table…? .

Fig. 5.8: Use of SST CTD in tent at L-2: setup in tent with fishing-rod and motor battery, water bottle and rope lying next to hole (left; photo Benjamin Rabe); SST CTD just before deployment with the fishing-rod (right; photo Steffen Graupner).

Lead events.

During Leg 2 team OCEAN participated in two lead events. Both time fishing-rod CTD was used. During one event portable version of MSS was also used. Data and positions of stations were stored in d-ship and MCS systems.

M-site T/S chain buoys.

8 T/S chains buoys by Pacific Gyre with 5 SBE SM37 (Microcat) CTD on each on were deployed at the M-sites during leg 1b under the project of sub-mesoscale dynamics of upper ocean. Details of the deployment and types of buoys could be found in report of leg 1b (see the Distributed Network cruise report). For inter calibration of these buoys flights operations with MSS and fishing-ctd were planned (once per leg at each cite). During dark conditions Leg

2 flight to M-cites were not possible due to absence of landing lights. Only one exceptional flight was performed during full moon conditions, when visibility (due to full moon) allowed to find M5 cite and land. Due to limitation in time (landed helicopter could wait up to 45 minutes on ice) one CTD profile with fishing-rod was performed. These data later will be used for comparison and calibration with M5 T/S chain.

Fig. 5.9 Use of fishing-rod CTD at M5-cite.

Data from buoys are transferred via satellite and stored at meersportal. During Leg 2 downloading data on regular base to the *Polarstern* were established. We also develop scripts for automatic post processing of these data. Later , downloaded data were automatically post processed on one of the linux Virtual Mashine (VM) on *Polarstern* (ip: 192.168.6.65) and resulted figures regularly (every hour, upon data availability) are uploading to the quicklooks. Figures showed dynamics of temperature and salinity on 5 depth from each of the buoys for deployment to current date and zoom to five last days. This fast look could give a hint for planning of OC work at short notice.

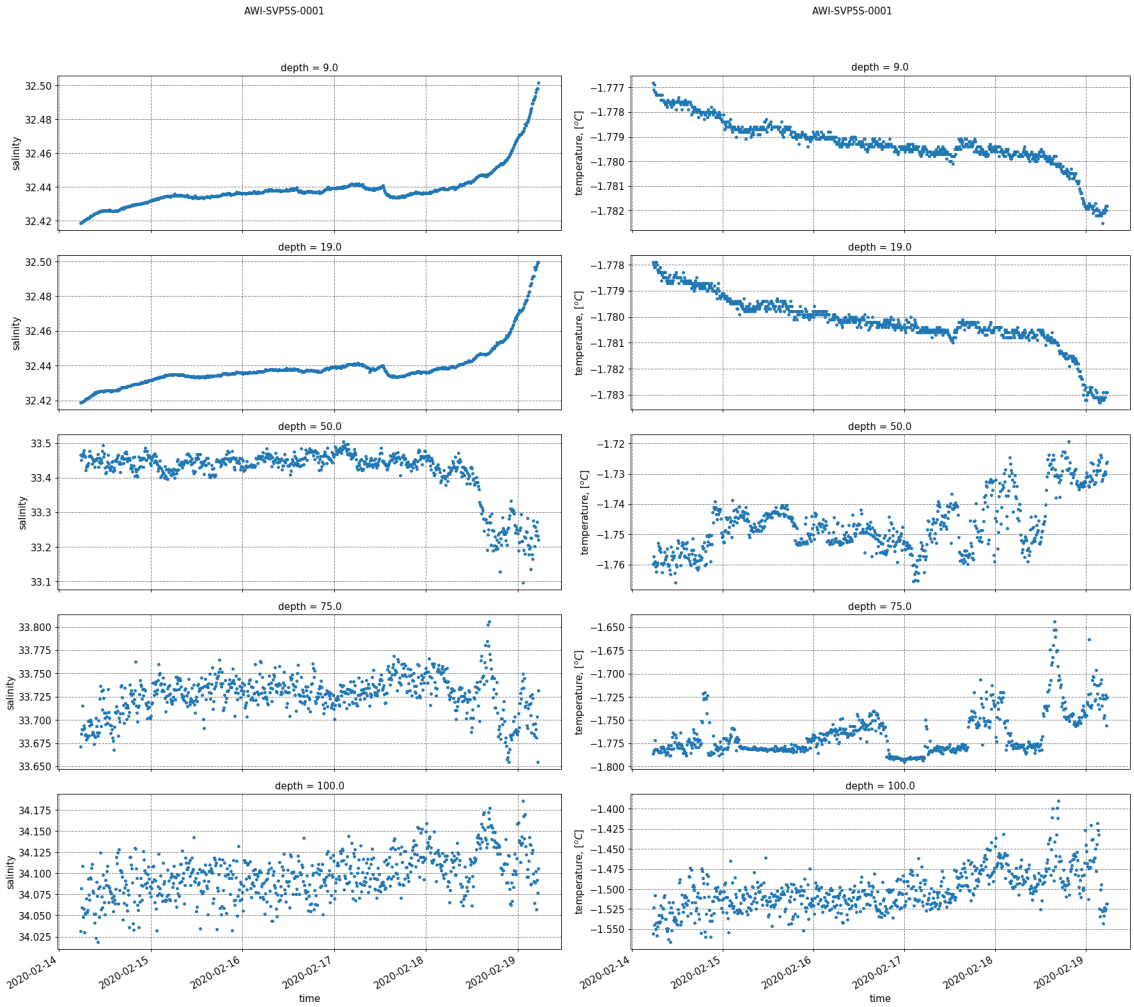
AWI-SVP5S-0001
AWI-SVP5S-0001
depth = 9.0
depth = 19.0
depth = 50.0
depth = 75.0
depth = 100.0
salinity
temperature, [°C]
time
2020-02-14
2020-02-15
2020-02-16
2020-02-17
2020-02-18
2020-02-19

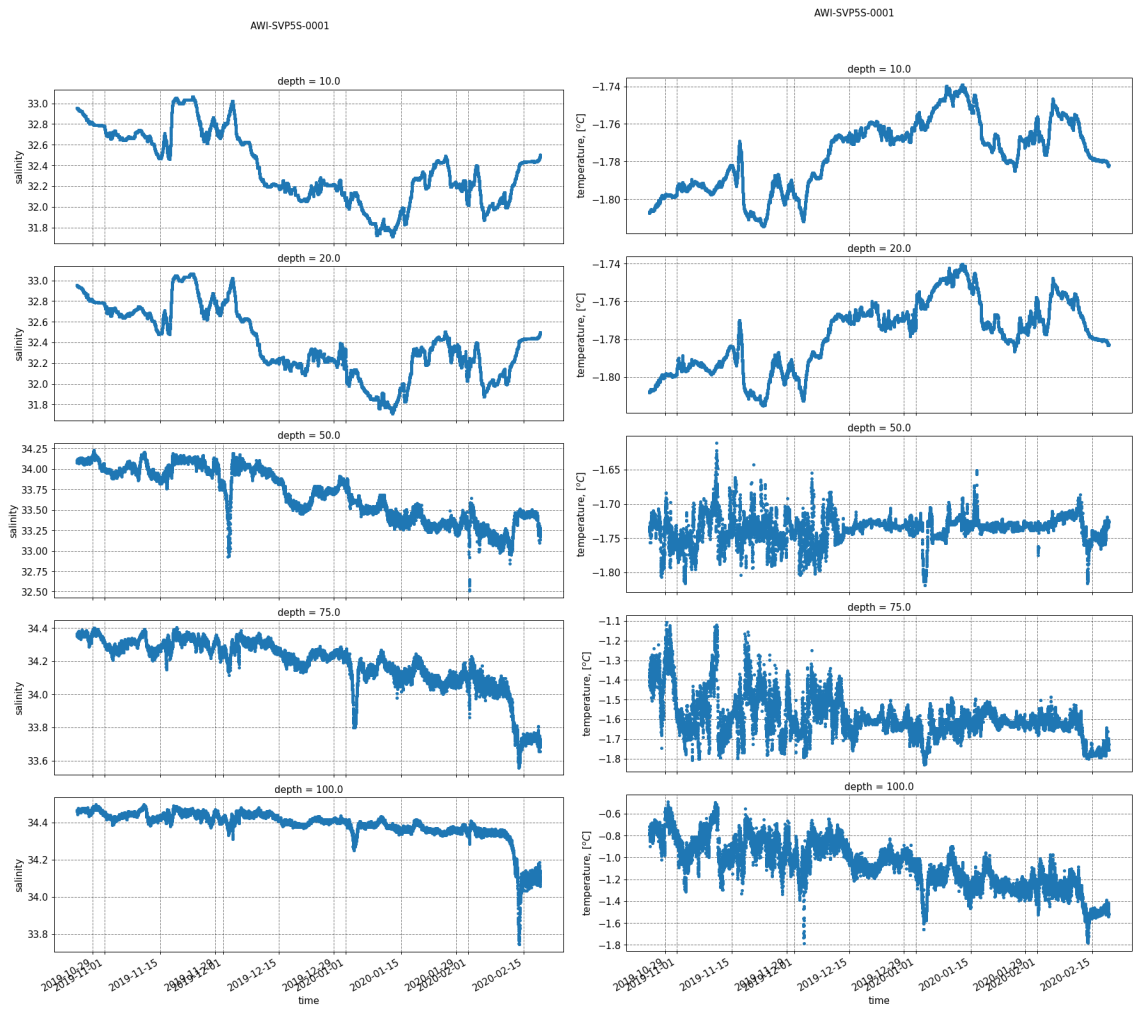

Fig. 5.10 Example of figures from M-cite buoys available at quicklooks. Figures automatically updating every hour (if new data are available).

Sampling for CFC/SF6, Helium & Tritium

All CFC/SF6, helium, and tritium samples during leg 2 were taken during the ship-based CTD operations. Sampling was also attempted in Ocean City during leg 1, but turned out to be challenging. Detailed report provided by Leg 1. Due to a high sample loss ratio and low quality of samples partly due to the absence of expertise together with unprepared procedure of sample transporting all sampling were done from PS CTD. On second week of Leg 2 laboratory equipment for flaming and preparation of ampules were transported from AWI013 container to "Mess- und Registrierraum" ("Drylab 5").

Ampoules for sampling CFC/SF6 and cleaning system were prepared one day prior to a deep CTD cast. Metal accessories of the ampoules were examined, rinsed, and cleaned before sampling. All sampling was carried out during the regular Thursday CTD operation deep-water casts. The naming convention for each sampled ampoule and metal tubes for Helium follows the D-Ship station id and continued after leg 1. For example, the samples taken on 9 November had the D-Ship station id PS122/1_6-81. A sample taken from bottle #1 closed at 3000 m for example had a label called PS122/1_6-81/1/3000. The same rules apply to sampled copper tubes and tritium bottles. Flamed ampoules and sampled copper tubes and tritium bottles were dried and then carefully stored in their original boxes. Information on CFC/Helium/(Tritium) samplings can be found in the corresponding log sheets and the corresponding electronic versions (Excel tables) in separated documents. Paper versions were left on board. Copper

tubes with Helium samples from Leg 1 and Leg 2 were transferred to Bremerhaven during the Leg 2/Leg 3 exchange. The sampling procedure was described in the provided SOP and not included in the current report. The water sampling strategy was reported during leg 2 in water budged excel sheets and provided in separate files.

AROMA turbulence moorings

In order to address its objectives, AROMA contributes 3 permanent installations on the main ice floe. These autonomous, continuous recording systems are planned to be operative in all legs. In addition, one vertical microstructure profiler is planned to be operated in coordination with the profiling from the Ocean City during all legs. Dissipation measurements in the upper 80 m up to the ice-water interface using this uprising vertical microstructure profiler will be crucial to resolve the under-ice boundary layer and to better quantify the ocean heat fluxes in the upper water column.

ADCP Longranger mooring, ocean thermistor chain and microrider mooring and cluster mooring were deployed during leg 1. During leg 2 regular data download and backup were carried out. For each instrument detailed instructions were prepared and transferred to leg 3. After deploying the ocean thermistor chain several of the sensors showed unrealistically high temperature. During Leg 2 the remainder of the temperature sensors were not functioning correctly (to high temperature) except one. The reason for sensor failure could not be determined. The microrider deployed together with the thermistor chain had issues with a corrupted SD memory card. Formatting the SD card resolved the problem. Data from all moorings were regularly downloaded and copied to the MCS. CTDs on cluster moorings started to report a critical battery level. After that no attempts were made to download data from those instruments. The SAMI had issues with the power supply. The mooring was inspected from the ROV by the ICE team. Details with photos and a video of these inspections were published in the MOSAiC logbook.

Installation of other platforms

Thermistor chain buoy (PI: Y. Kawaguchi)

A thermistor chain of the type IceBTC60 with 17 thermistors on 60 m cable at 2-5 m spacing was deployed close to Ridge area (see ice floe map) on 11 January 2020 (see Figs 5.). Near-real time temperature data of the water column is reported back via Iridium on a regular interval. The deployment is part of the project “Measurement of lee waves and turbulent heat flux behind ice keels in ice-ocean boundary layer” of the University of Tokyo.

Figure 5.11 Deployment of the IceBTC60 on the Ridge.

T-POP deployment (PI: C. Heuze)

The T-POP is a football-sized autonomous temperature sensor that sits at the bottom of the ocean for a pre-set time, taking measurements every hour. It then automatically burns its anchoring link to float back to the surface and send its data by satellite. Five out of a total of ~25 of such sensors were deployed during Leg 2 after two near-bottom CTD profiles (see Fig. 5.). These sensors are part of the project "*Why is the deep Arctic Ocean Warming? (WAOW)*" of the University of Gothenburg. The T-POP will quantify for the first time the high frequency, seasonal and interannual variability of the deep Arctic Ocean temperature. This variability quantification is required for putting into context the MOSAiC and historical point measurements of the CTD. Team OCEAN had deployed five T-POPs. Preparation and deployment usually been done by one person.

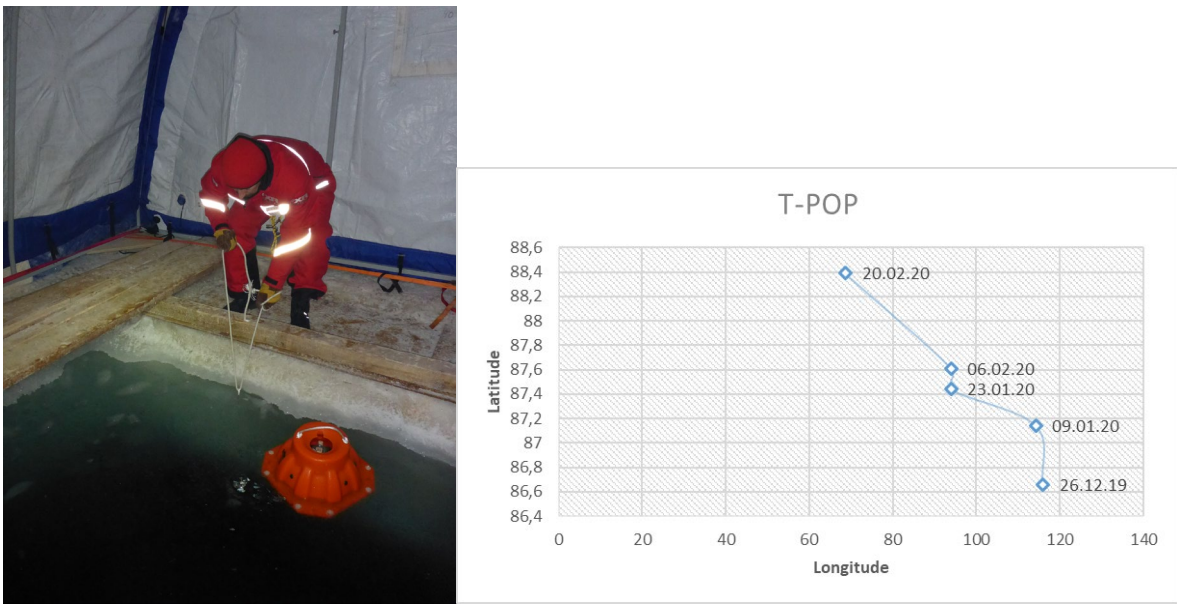

Fig. 5.12: Left: Deployment of T-POP profiler in PS ice hole (photo by Eric Brossier). Right: Positions and date of T-POP deployment.

Thermistor chain network (PI: Mario Hoppmann)

Please see Team Ice chapter.

GPS ridge tracker buoys (PI: Y. Kawaguchi)

GPS trackers buoy were prepared by OCEAN team and deployed by ICE team. For details of the deployment see Team Ice chapter and MOSAiC logbook entries.

Preliminary (expected) results

Water masses and regional ocean environment

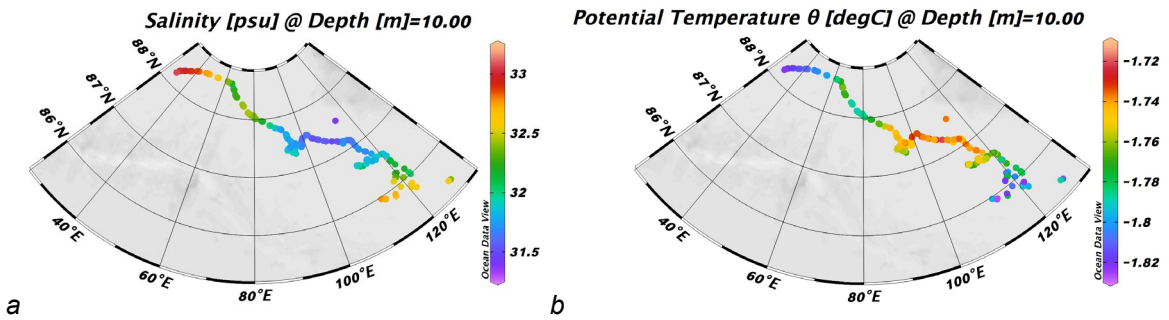

Fig. 5.13: Practical salinity (a) and potential temperature (referenced to 0 dbar), θ, (b) at 10 m depth from all CTD observations throughout legs 1 and 2.

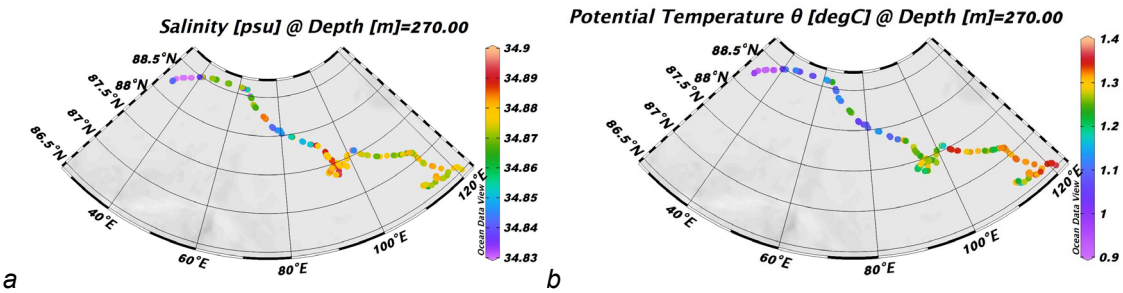

Fig. 5.14: Practical salinity (a) and θ (b) at 270 m depth from the same data as in Figure 5.13.

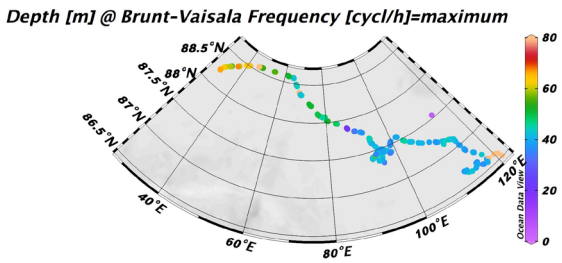

Fig. 5.15: Depth of the maximum buoyancy frequency, approximating mixed-layer depth, from the same data as in Figure 5.13.

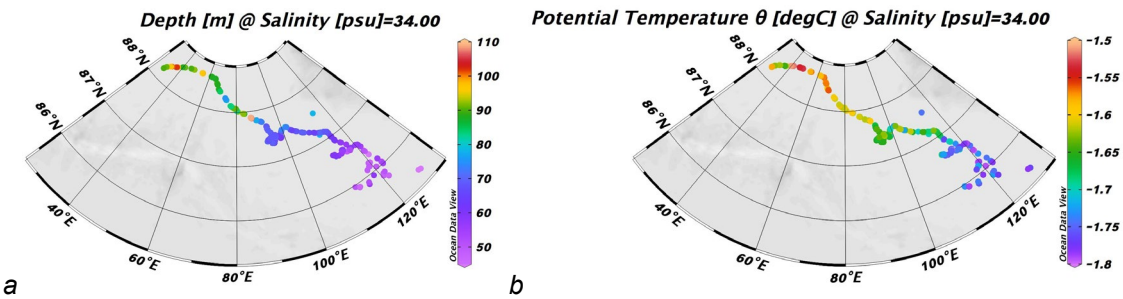

Fig. 5.16: Depth (a) and θ (b) at a practical salinity of 34 from the same data as in Figure 5.13.

Potential temperature (θ, referenced to 0 dbar) and practical salinity during the drift of legs 1 and 2 Polarstern from about 86.5 °N, 120 °E to 88.6 °N, 60 °E and subsequent drift toward the southwest during the early part of leg 3, are shown for selected depths in Figures 5.13 to 5.14.

The practical salinity at 10 m depth (Figure 5.13 a) showed a decrease in practical salinity with latitude to about 87 °N, 100 °E, in about mid-January. Further on practical salinity increased again until the end of leg 2. This can be explained by superposition of a cross-Arctic gradient in near-surface salinity, freshening along the cruise track, and continuous brine release due to seasonal ice formation. Overall, practical salinity is close to that of the inflowing Atlantic Water near the Barents Sea shelf and below 30 in the Beaufort Gyre, north of North America. After about mid-January, the brine release appears to dominate changes in practical salinity in the upper mixed-layer.

The mixed-layer depth, approximately represented in Figure 5.15 (a) by the depth of the maximum in the buoyancy frequency in each profile, increases more of less continuously from values just under 40 m early in leg 1 to above 60 m near the end of leg 2. The one obvious exception are values relatively low compared to the surrounding profiles around 87.9 °N due to a passing eddy on 12 February. The eddy showed higher salinity in the lower part of the mixed-layer, shown by surrounding profiles, and lower salinity in the upper and parts of the lower halocline (profiles not shown). The nature of the anomalous feature was confirmed to be an eddy by velocity observations of the various ADCP around the CO.

The warm Atlantic Water around 270 m depth overall cooled and freshened along the cruise track toward the northwest, albeit with some smaller scale variability (Figure 5.14). This could be due to slow diffusive processes along the pathways of the warm Atlantic Water from the boundary current near the continental slope via the Gakkel and Lomonosov ridges toward the inner basin. On the other hand, the temperature and salinity of the warm Atlantic Water is indicative of the pathways this water had taken into the Arctic Ocean, either through the Barents Sea or through the Fram Strait (e.g. Rudels, B.; 2009).

The depth of the lower halocline (Figure 5.16 a), taken to be around a practical salinity of 34 (e.g. Rudels et al., 2004), became deeper throughout, from being just underneath the mixed-layer near the beginning of leg 1 to around 100 m toward the end of the cruise track. The temperature in the lower halocline increased along the cruise track. This marks the origin of the lower halocline, where the southern part is close to the boundary current near the continental slope of the Barents, Kara and Laptev seas, where the lower halocline is generated after the inflow of warm Atlantic Water via the Fram Strait by consecutive winter haline convection and melt (c.f. “Atlantification”; Polyakov et al., 2017). The corresponding temperature in the lower halocline is close to the freezing point. The profiles further north show a lower halocline characteristic of that created in the Barents Sea, where enhanced mixing of at the continental slope with warm Atlantic Water leads to temperatures significantly warmer than freezing (see e.g. Rudels et al., 2009). In addition, is likely due to slow diffusive processes are likely to act onalong the halocline pathways into the inner basin.,

There are no clear signs of waters of Pacific origin.

The above will be detailed further in a comprehensive water mass analysis in the future, in combination with different tracer samples taken from the CTD/rosette.

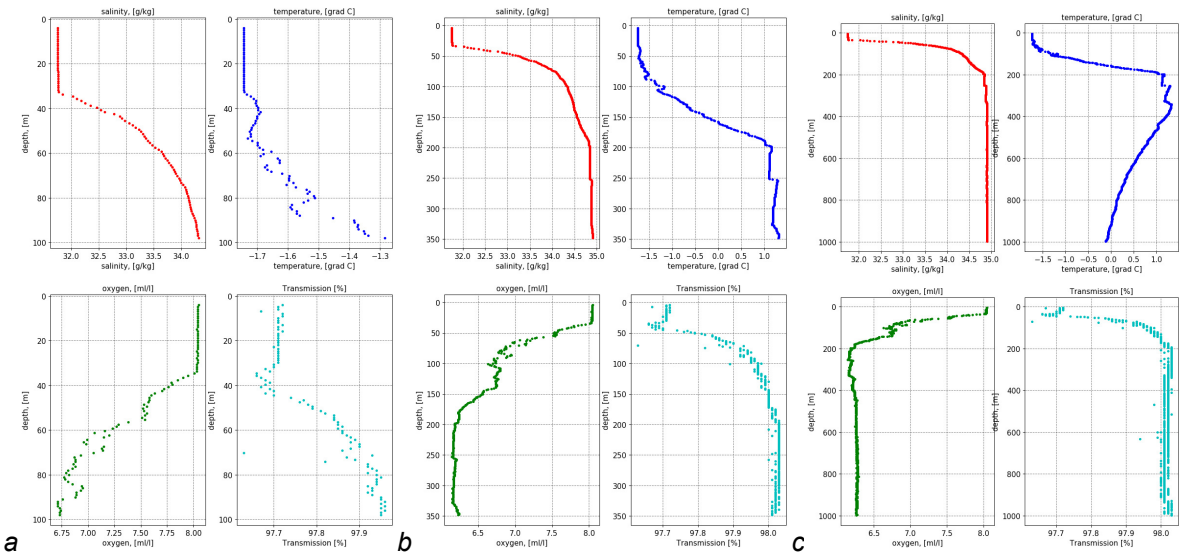

Figure 5.17: Example of CTD cast preliminary overview uploaded to quicklooks for other teams use.

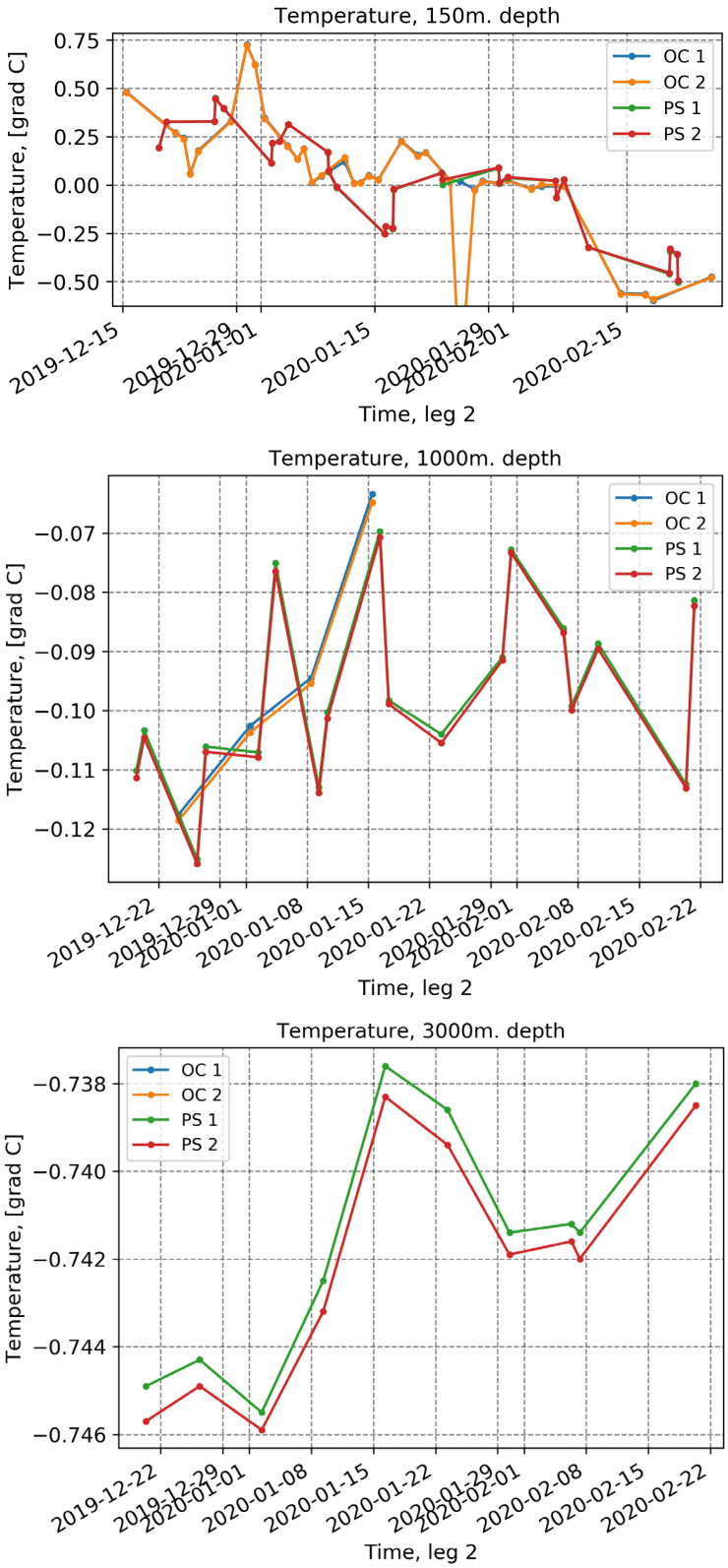

Figure 5.18: Comparison of salinity and temperature from OC and PS CTDs for 2 sensors each.

Additional inter-calibrations of PS and OC CTD sensors is needed. In the middle of January 2020, sensor of OC start to deviate from each other, additional attention is need for these data. Moreover, it could be a suggestion for later legs to change OC sensor set 2.

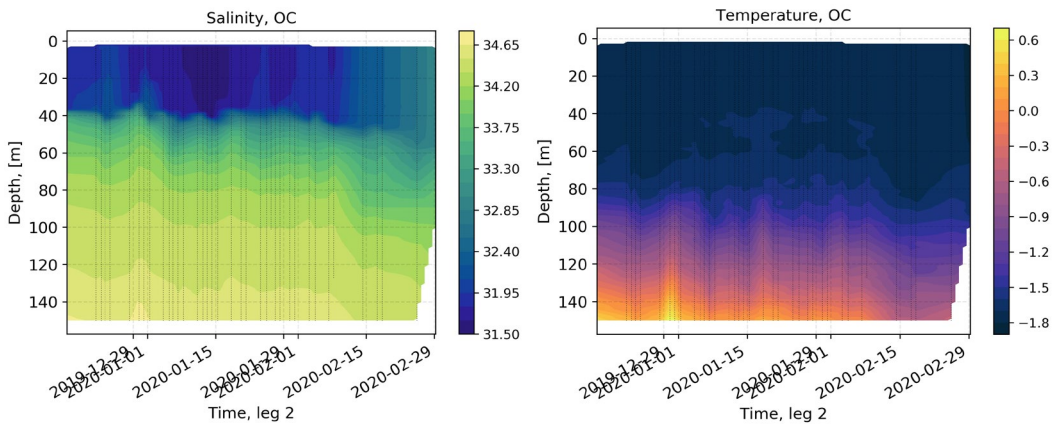

Figure 5.19: Time series of salinity and temperature (0 – 150 meters depth) from OC CTD during Leg 2.

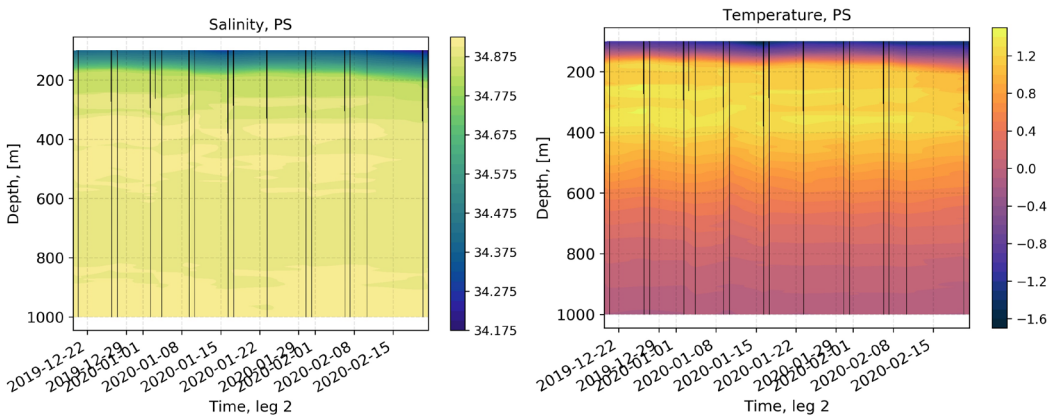

Figure 5.20: Time series of salinity and temperature (100 – 1000 meters depth) from PS during Leg 2.

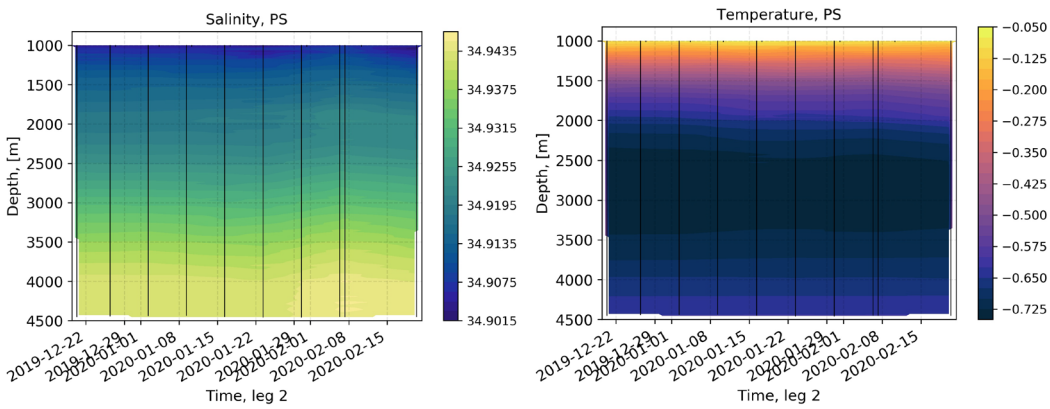

Figure 5.21Time series of salinity and temperature (1000 – 4500 meters depth) from PS during Leg 2 drift.

Turbulent mixing in the upper water column

During Leg 2 of MOSAiC the turbulence observations covered the central region of the Amudsen Basin in the Central Arctic Ocean between 86.5°N and 88.5°N. This location is far from any shelf. Current speeds are generally low, and mostly barotropic. Due to the high

latitude tidal forcing is mostly negligible. Main source for turbulent kinetic energy (TKE) in the upper water column is the shear stress between the drifting ice and the underlying water.

The upper part of the ocean is strongly stratified in temperature and salinity. Below the well mixed upper layer of 30 to 50m thickness, a strong increase in salinity form a cold halocline layer on top of the underlying water of Atlantic origin. The temperature is strongly increasing in the transition between the cold halocline and the core of the warm Atlantic Water, which was found between 200 and 400m depth. However, the strongest density interface was found at the bottom of the mixed layer (Figure 5.16). From 1st November until the beginning of leg 2 on 15th December 2019 the mixed layer depth increased from about 25m to 35m. Concurrent with the deepening of the mixed layer the strength of density stratification increased. This process was slowing down during leg 2. From mid-January until mid-February the mixed layer depth increased only slightly to about 40 to 45m. After the passage of a mesoscale eddy on 12th February (see also Figure 5.22) the density stratification at the bottom of the mixed layer decreased significantly.

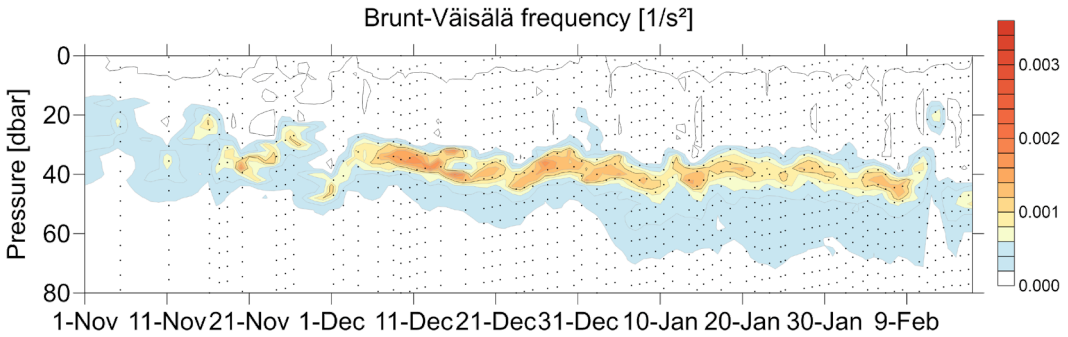

Figure 5.22: Time series of Brunt-Väisälä frequency, derived from daily averaged MSS profiles. The figure covers Leg1 and 2 of MOSAiC.

During the entire observation period the mixed layer temperature was close to freezing point or slightly below (Figure 5.23). The weak temperature gradient in the cold halocline points to low heat fluxes from into the mixed layer.

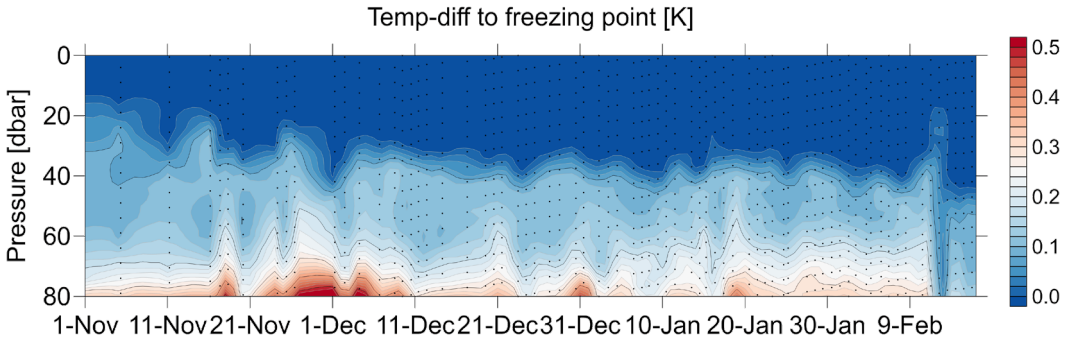

Figure 5.23: Time series of temperature deviation from freezing point, derived from daily averaged MSS profiles. The figure covers Leg1 and 2 of MOSAiC.

The primary purpose of the MSS measurements was to gather information about turbulent mixing at the ice – ocean interface. The main source for TKE in the upper layer is the shear stress between the drifting ice and the underlying water column. The strong density stratification at the base of the surface mixed layer limits the downward propagation of TKE.

Below the strong pycnocline at 30 to 45m the TKE dissipation rate was close or below the noise level of the instrument (Figure 5.24, lower panel). The obvious decrease in dissipation rate below the pycnocline mid- December is an artificial signal, caused be the reduction of instruments noise level due to reduced sinking velocity. In the surface mixed layer the TKE dissipation is clearly correlated to the drift velocity of the ice floe (Figure 5.24). Highest TKE dissipation rates were detected closest to the ice. Generally, the TKE dissipation decreased down wards. A secondary maximum was often observed at the bottom of the mixed layer.

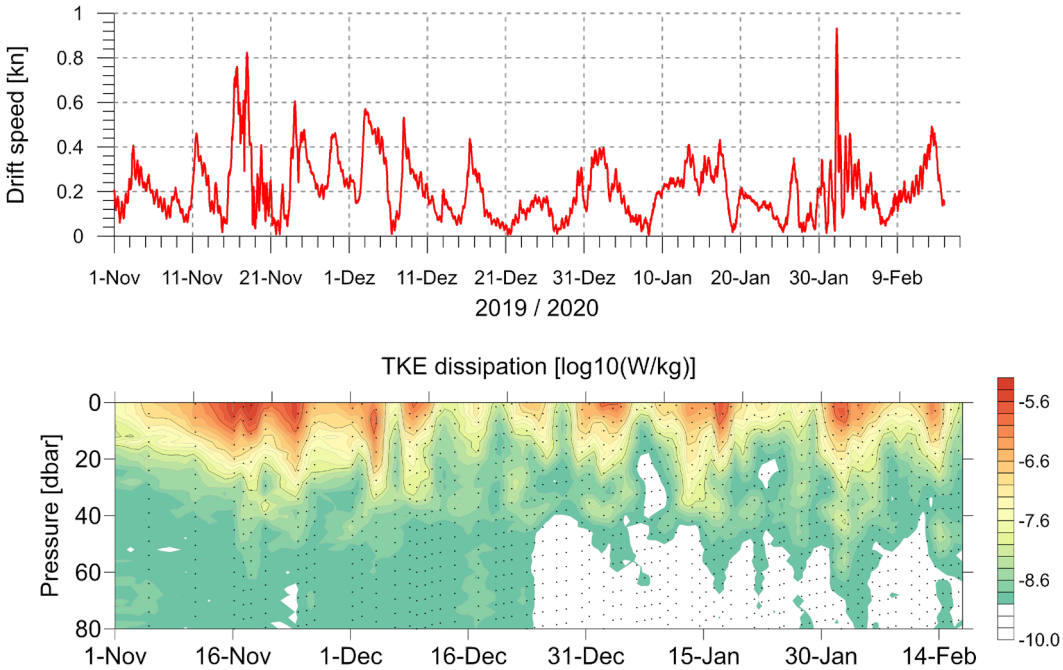

Figure 5.24: Timer series of drift velocity of the ice floe (upper panel) and dissipation rate of turbulent kinetic energy (TKE) in the upper 60m (lower panel). Plots derived from daily averaged MSS profiles. The figure covers Legs1 and 2 of MOSAiC.

Below the mixed layer the mixing is dominated by double diffusive processes. Figure 5.25 depict the time series of Turner angle that characterizes the type of double diffusive mixing. In the cold halocline between 50 and 100m, the temperature stratification is unstable and weak convective overturns can be expected. In the upper thermocline of the warm Atlantic Water (AW) between 100 and 180m pronounced double diffusive staircases were observed throughout the observation period. In the core of AW deeper than 180 m salt fingering is the dominating process. Three layers of salt fingering were separated by a shallow layer with unstable temperature stratification and thermohaline staircases.

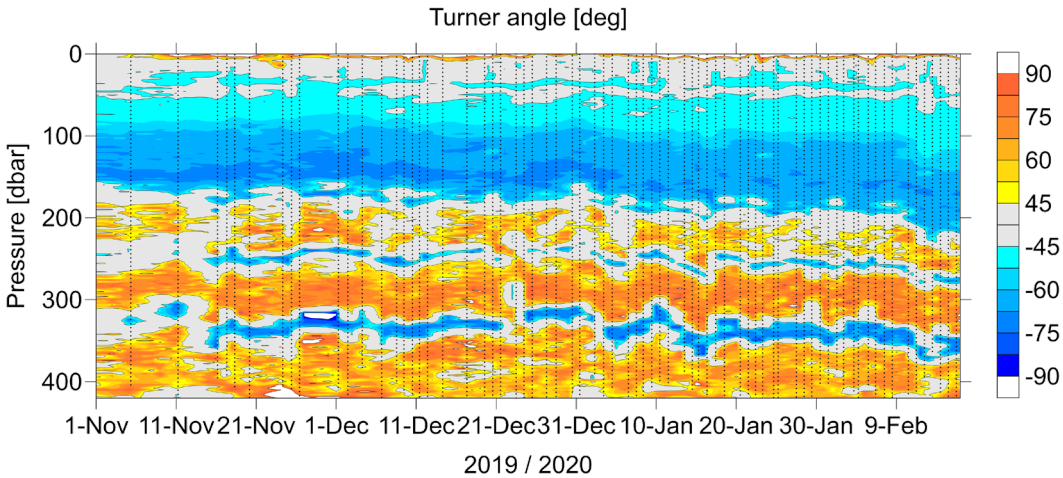

Figure 5.25: Timer series of Turner angle in the upper 400m along the drift path. Blue areas are dominated by double diffusive convective overturns. Double diffusive salt fingering dominates in yellow to red areas. Data derived from daily averaged MSS profiles. The figure covers Legs 1 and 2 of MOSAiC.

Current measurements

The current measurements carried out with the SADCP of *Polarstern* cover the upper 220 to 240m. The observed current speed was generally weak, on average in the range of 0.02 to 0.04 ms^{-1}. Figure 5.20 depicts a fifteen days section of the entire time series. Superimposed to the weak barotropic background current, internal waves of inertial period are visible throughout the covered depth range. Around day 7 of the depicted section the drifting floe passed a mesoscale eddy. Its core was located between 30 and 120m water depth. Assuming a low background velocity, the diameter of the eddy was estimated with 10 to 15 nautical miles. The highest observed velocities inside the eddy was about 0.3 ms^{-1}. The frequency of passing eddies along the drift path was about one eddy per month.

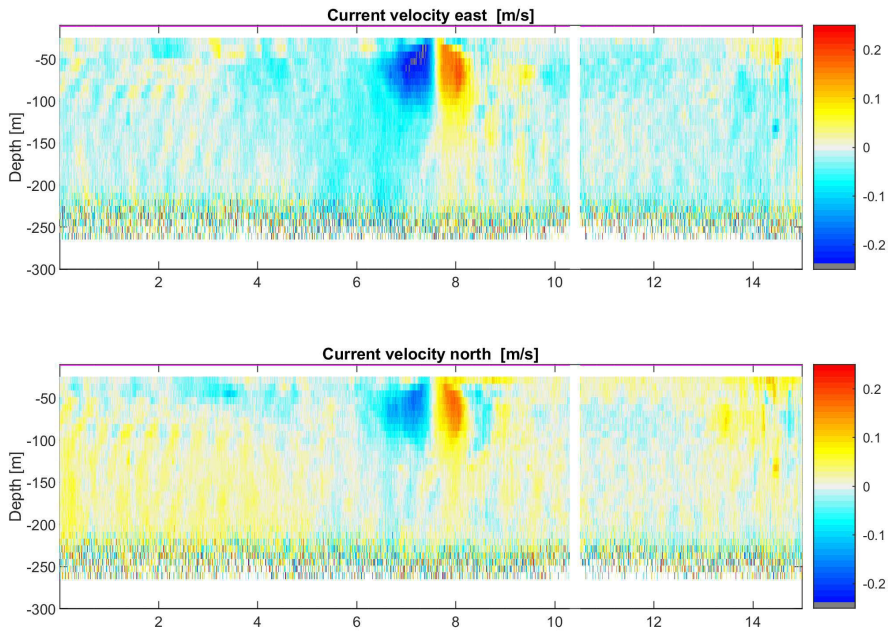

Figure 5.26: Current components measured with the SADCP of Polarsterrn. (Time in days after the 5th February 2020)

Preliminary (expected) results LISST

One year-round data of suspended particles are expected to be obtained by continuously deploying LISST instrument during entire MOSAiC expedition. Spatial and temporal variations of particles in different seasons as well as physical, chemical and biological processes in the water column will be recorded and analyzed to estimate the sources and dynamics of suspended particles as well as interactions with ecosystems over the central Arctic Ocean.

Figure 5.28 shows particle volume concentration of suspended particulate matter captured by LISST. Vertical distribution demonstrates between 50m and 100m the concentration reaches its peak. At the other levels the concentration is limited around only 0.3 µl/l. The temporal variation suggests the particle volume concentration of suspended particulate matter in February is significantly increased compared with the values in November and December which are less than 0.2 µl/l。

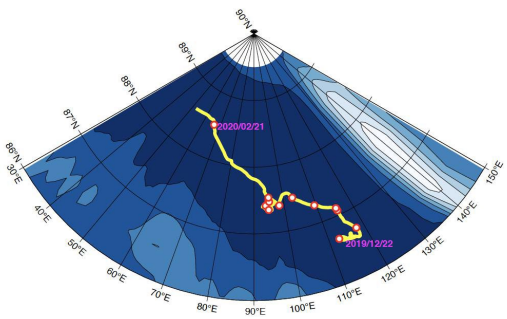

Fig. 2.27 Map of LISST profiling stations in the central Arctic Ocean. Yellow line indicates the track on sea ice from December 16 2019 to February 24 2020 during the MOSAiC expedition.

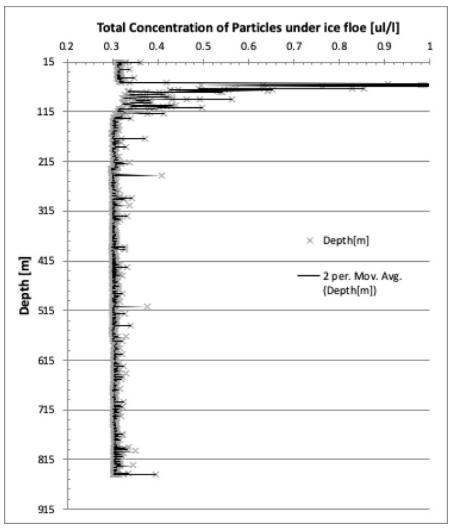

Fig.5.28 Example of profile of total particle volume concentration distribution.

Data management

All data are handled, documented, archived and published following the MOSAiC data policy (see APPENDIX).

References

Koch BP, Dittmar T (2006) From mass to structure: An aromaticity index for high-resolution mass data of natural organic matter. Rapid communications in mass spectrometry, 20, 926-932.

Alford, M. H., MacKinnon, J. A., Simmons, H. L., & Nash, J. D. (2016). Near-Inertial Internal Gravity Waves in the Ocean. *Annual Review of Marine Science*, *8*, 95–123. https://doi.org/10.1146/annurev-marine-010814-015746

Bebieva, Y., & Timmermans, M.-L. (2015). An examination of double-diffusive processes in a mesoscale eddy in the Arctic Ocean. *Journal of Geophysical Research: Oceans*, *121*(1), 457–475. https://doi.org/doi:10.1002/2015JC011105

D'Asaro, E. A., & Morehead, M. D. (1991). Internal waves and velocity fine structure in the Arctic Ocean. *Journal of Geophysical Research: Oceans*, *96*(C7), 12725–12738. https://doi.org/10.1029/91JC01071

Guthrie, J. D., Morison, J. H., & Fer, I. (2013). Revisiting internal waves and mixing in the Arctic Ocean. *Journal of Geophysical Research: Oceans*, *118*(8), 3966–3977. https://doi.org/10.1002/jgrc.20294

Halle, C., & Pinkel, R. (2003). Internal wave variability in the Beaufort Sea during the winter of 1993/1994. *Journal of Geophysical Research: Oceans*, *108*(C7), n/a-n/a. https://doi.org/10.1029/2000JC000703

Manucharyan, G. E., & Thompson, A. F. (2017). Submesoscale Sea Ice-Ocean Interactions in Marginal Ice Zones. *Journal of Geophysical Research: Oceans*, *122*(12), 9455–9475. https://doi.org/10.1002/2017JC012895

Morison, J. H., Long, C. E., & Levine, M. D. (1985). Internal wave dissipation under sea ice. *Journal of Geophysical Research: Oceans*, *90*(C6), 11959–11966. https://doi.org/10.1029/JC090iC06p11959

Polyakov, I. V., Pnyushkov, A. V., Rember, R., Ivanov, V. V., Lenn, Y.-D., Padman, L., & Carmack, E. C. (2012). Mooring-Based Observations of Double-Diffusive Staircases over the Laptev Sea Slope*. *Journal of Physical Oceanography*, *42*(1), 95–109. https://doi.org/10.1175/2011JPO4606.1

Polyakov, I. V, Pnyushkov, A. V, Alkire, M. B., Ashik, I. M., Baumann, T. M., Carmack, E. C., et al. (2017). Greater role for Atlantic inflows on sea-ice loss in the Eurasian Basin of the Arctic Ocean. *Science*, *356*(6335), 285–291. https://doi.org/10.1126/science.aai8204

Proshutinsky, A. Y., & Johnson, M. A. (1997). Two circulation regimes of the wind-driven Arctic Ocean. *Journal of Geophysical Research: Oceans*, *102*(C6), 12493–12514. https://doi.org/doi:10.1029/97JC00738

Rabe, B, Heuzé, C, Regnery, J, Aksenov, Y, Allerholt, J, Athanase, M, Bai, Y, Basque, C, Bauch, D, Baumann, TM, Chen, D, Cole, ST, Craw, L, Davies, A, Damm, E, Dethloff, K, Divine, DV, Doglioni, F, Ebert, F, Fang, Y-C, Fer, I, Fong, AA, Gradinger, R, Granskog, MA, Graupner, R, Haas, C, He, H, He, Y, Hoppmann, M, Janout, M, Kadko, D, Kanzow, T, Karam, S, Kawaguchi, Y, Koenig, Z, Kong, B, Krishfield, RA, Krumpen, T, Kuhlmey, D, Kuznetsov, I, Lan, M, Laukert, G, Lei, R, Li, T, Torres-Valdés, S, Lin, L, Lin, L, Liu, H, Liu, N, Loose, B, Ma, X, MacKay, R, Mallet, M, Mallett, RDC, Maslowski, W, Mertens, C, Mohrholz, V, Muilwijk, M, Nicolaus, M, O'Brien, JK, Perovich, D, Ren, J, Rex, M, Ribeiro, N, Rinke, A, Schaffer, J, Schuffenhauer, I, Schulz, K, Shupe, MD, Shaw, W, Sokolov, V, Sommerfeld, A, Spreen, G, Stanton, T, Stephens, M, Su, J, Sukhikh, N, Sundfjord, A, Thomisch, K, Tippenhauer, S, Toole, JM, Vredenborg, M, Walter, M, Wang, H, Wang, L, Wang, Y, Wendisch, M, Zhao, J, Zhou, M, Zhu, J. 2022. Overview of the MOSAiC expedition: Physical oceanography. *Elementa: Science of the Anthropocene* 10(1). DOI: https://doi.org/10.1525/elementa.2021.00062

Rudels, B., Schauer, U., Björk, G., Korhonen, M., Pisarev, S., Rabe, B., & Wisotzki, A. (2013). Observations of water masses and circulation with focus on the Eurasian Basin of the Arctic Ocean from the 1990s to the late 2000s. *Ocean Science*, *9*(1), 147–169. https://doi.org/10.5194/os-9-147-2013

Rudels, B., Korhonen, M., Schauer, U., Pisarev, S., Rabe, B., & Wisotzki, A. (2015). Circulation and transformation of Atlantic water in the Eurasian Basin and the contribution of the Fram Strait inflow branch to the Arctic Ocean heat budget. *Progress in Oceanography*, *132*, 128–152. https://doi.org/10.1016/j.pocean.2014.04.003

Timmermans, M.-L., Proshutinsky, A., Krishfield, R. A., Perovich, D. K., Richter-Menge, J. A., Stanton,

T. P., & Toole, J. M. (2011). Surface freshening in the Arctic Ocean's Eurasian Basin: An apparent consequence of recent change in the wind-driven circulation. *Journal of Geophysical Research: Oceans*, *116*(C8). https://doi.org/doi:10.1029/2011JC006975

Timmermans, Mary-Louise, Cole, S., & Toole, J. (2012). Horizontal Density Structure and Restratification of the Arctic Ocean Surface Layer. *Journal of Physical Oceanography*, *42*(4), 659–668. https://doi.org/10.1175/JPO-D-11-0125.1

Appendix

Tab. 5.6: CTD casts in Ocean City during MOSAiC Leg 2.

Dship Activity	Device	Date	aprox. Time	Longitude	Latitude	aprox. Depth
PS122/3_30-9	**CTD_SBE9plus_935**	2020-03-02	11:34:55	88,186737	31,077774	-
PS122/3_29-74	**CTD_SBE9plus_935**	2020-02-29	06:45:58	88,289575	32,234491	100
PS122/3_29-8	**CTD_SBE9plus_935**	2020-02-25	12:23:01	88,559956	45,651351	240
PS122/2_25-79	**CTD_SBE9plus_935**	2020-02-21	13:59:52	88,512263	66,286105	-
PS122/2_25-26	**CTD_SBE9plus_935**	2020-02-18	06:39:06	88,09121	77,68365	250
PS122/2_25-4	**CTD_SBE9plus_935**	2020-02-17	06:48:00	88,072534	79,219024	250
PS122/2_24-47	**CTD_SBE9plus_935**	2020-02-14	06:56:09	88,015513	80,765143	260
PS122/2_23-97	**CTD_SBE9plus_935**	2020-02-08	07:29:20	87,669254	93,859332	125
PS122/2_23-70	**CTD_SBE9plus_935**	2020-02-07	07:13:09	87,637158	93,753712	200
PS122/2_23-17	**CTD_SBE9plus_935**	2020-02-04	12:36:57	87,481599	95,325039	400
PS122/2_23-4	**CTD_SBE9plus_935**	2020-02-03	06:30:29	87,408738	93,196736	350
PS122/2_22-71	**CTD_SBE9plus_935**	2020-01-31	06:34:00	87,438138	96,478191	400
PS122/2_22-49	**CTD_SBE9plus_935**	2020-01-30	06:46:45	87,477255	96,275367	200
PS122/2_22-18	**CTD_SBE9plus_935**	2020-01-28	07:30:06	87,452348	95,820209	250
PS122/2_22-3	**CTD_SBE9plus_935**	2020-01-27	06:57:03	87,444826	95,608684	350
PS122/2_21-128	**CTD_SBE9plus_935**	2020-01-26	13:08:45	87,417148	93,882495	100
PS122/2_21-114	**CTD_SBE9plus_935**	2020-01-25	13:00:18	87,402696	92,829674	400
PS122/2_21-101	**CTD_SBE9plus_935**	2020-01-24	07:32:28	87,423262	93,193196	400
PS122/2_21-26	**CTD_SBE9plus_935**	2020-01-21	06:44:00	87,486169	96,413773	250
PS122/2_21-1	**CTD_SBE9plus_935**	2020-01-20	06:46:33	87,439898	97,610131	300
PS122/2_20-109	**CTD_SBE9plus_935**	2020-01-18	08:00:55	87,411213	98,292891	350
PS122/2_20-32	**CTD_SBE9plus_935**	2020-01-15	12:36:44	87,477876	103,15939	1000
PS122/2_20-17	**CTD_SBE9plus_935**	2020-01-14	06:47:44	87,399528	105,34836	250
PS122/2_20-2	**CTD_SBE9plus_935**	2020-01-13	06:51:13	87,318476	107,6282	370
PS122/2_19-123	**CTD_SBE9plus_935**	2020-01-12	11:30:39	87,275083	109,41506	500
PS122/2_19-89	**CTD_SBE9plus_935**	2020-01-11	06:39:43	87,210628	111,40559	350
PS122/2_19-42	**CTD_SBE9plus_935**	2020-01-08	11:00:45	87,112754	115,19703	1000
PS122/2_19-18	**CTD_SBE9plus_935**	2020-01-07	07:17:52	87,121507	114,93465	250
PS122/2_19-4	**CTD_SBE9plus_935**	2020-01-06	07:16:51	87,099651	115,2478	500
PS122/2_18-91	**CTD_SBE9plus_935**	2020-01-05	13:24:48	87,072431	115,31747	500
PS122/2_18-81	**CTD_SBE9plus_935**	2020-01-04	07:55:55	86,993012	115,44657	500
PS122/2_18-25	**CTD_SBE9plus_935**	2020-01-01	12:42:23	86,709316	117,91846	1100
PS122/2_18-16	**CTD_SBE9plus_935**	2019-12-31	06:51:34	86,580904	117,8117	250
PS122/2_18-5	**CTD_SBE9plus_935**	2019-12-30	07:42:06	86,605802	116,62123	500
PS122/2_17-78	**CTD_SBE9plus_935**	2019-12-28	06:50:07	86,675622	115,7679	500
PS122/2_17-18	**CTD_SBE9plus_935**	2019-12-24	08:57:18	86,625595	113,80698	1000
PS122/2_17-7	**CTD_SBE9plus_935**	2019-12-23	08:03:11	86,645239	113,08542	500

PS122/2_16-64	**CTD_SBE9plus_935**	2019-12-22	12:22:54	86,670643	112,64924	500
PS122/2_16-54	**CTD_SBE9plus_935**	2019-12-21	12:48:17	86,687124	112,39831	250
PS122/2_16-94	**CTD_SBE9plus_935**	2019-12-15	11:19:37	86,619083	117,97366	200

Tab. 5.7: CTD casts using the ship-based CTD/Rosette system during MOSAiC Leg 2.

Dship Activity	Device	Date	aprox. Time	Longitude	Latitude	aprox. Depth
PS122/2_25-73	**CTD_SBE9plus_321**	2020-02-21	08:51:16	88,489366	66,707383	1000
PS122/2_25-71	**CTD_SBE9plus_321**	2020-02-21	06:20:43	88,477994	66,960834	300
PS122/2_25-54	**CTD_SBE9plus_321**	2020-02-20	12:15:52	88,390997	68,60682	4360
PS122/2_25-52	**CTD_SBE9plus_321**	2020-02-20	06:47:14	88,365214	69,441689	330
PS122/2_24-4	**CTD_SBE9plus_321**	2020-02-10	08:44:27	87,782439	91,897737	1000
PS122/2_24-2	**CTD_SBE9plus_321**	2020-02-10	06:20:04	87,77732	92,030733	100
PS122/2_23-63	**CTD_SBE9plus_321**	2020-02-07	10:06:48	87,640085	93,772332	4360
PS122/2_23-47	**CTD_SBE9plus_321**	2020-02-06	12:20:43	87,61157	93,953292	4360
PS122/2_23-46	**CTD_SBE9plus_321**	2020-02-06	06:48:00	87,597838	94,063437	300
PS122/2_22-63	**CTD_SBE9plus_321**	2020-01-31	09:53:25	87,452288	96,402555	1000
PS122/2_22-47	**CTD_SBE9plus_321**	2020-01-30	12:02:00	87,45572	96,538858	4360
PS122/2_22-42	**CTD_SBE9plus_321**	2020-01-30	06:48:40	87,477193	96,27755	300
PS122/2_21-65	**CTD_SBE9plus_321**	2020-01-23	12:29:34	87,439603	93,923956	4360
PS122/2_21-64	**CTD_SBE9plus_321**	2020-01-23	06:47:50	87,448149	94,132803	320
PS122/2_20-73	**CTD_SBE9plus_321**	2020-01-17	09:21:33	87,514125	99,40755	1000
PS122/2_20-71	**CTD_SBE9plus_321**	2020-01-17	06:33:40	87,53075	99,621063	280
PS122/2_20-46	**CTD_SBE9plus_321**	2020-01-16	11:39:44	87,562446	101,5487	4360
PS122/2_20-45	**CTD_SBE9plus_321**	2020-01-16	06:54:50	87,55461	101,98932	380
PS122/2_19-77	**CTD_SBE9plus_321**	2020-01-10	08:59:19	87,172095	112,92965	1000
PS122/2_19-76	**CTD_SBE9plus_321**	2020-01-10	06:25:40	87,167872	113,10756	100
PS122/2_19-56	**CTD_SBE9plus_321**	2020-01-09	11:34:17	87,14406	114,26063	4350
PS122/2_19-55	**CTD_SBE9plus_321**	2020-01-09	06:43:01	87,136615	114,5361	300
PS122/2_18-74	**CTD_SBE9plus_321**	2020-01-04	10:38:13	87,001941	115,41496	1000
PS122/2_18-57	**CTD_SBE9plus_321**	2020-01-03	06:38:26	86,898882	115,74118	260
PS122/2_18-34	**CTD_SBE9plus_321**	2020-01-02	13:08:46	86,832392	116,50168	4350
PS122/2_18-32	**CTD_SBE9plus_321**	2020-01-02	07:45:28	86,804435	116,86732	290
PS122/2_17-68	**CTD_SBE9plus_321**	2019-12-27	11:01:49	86,67859	115,95642	1000
PS122/2_17-64	**CTD_SBE9plus_321**	2019-12-27	07:02:56	86,67642	115,99108	100
PS122/2_17-41	**CTD_SBE9plus_321**	2019-12-26	13:28:07	86,65544	115,91842	4350
PS122/2_17-39	**CTD_SBE9plus_321**	2019-12-26	07:16:03	86,648052	115,72748	270
PS122/2_16-34	**CTD_SBE9plus_321**	2019-12-20	12:16:30	86,680364	112,56835	4360
PS122/2_16-21	**CTD_SBE9plus_321**	2019-12-19	11:50:27	86,67829	112,95509	1000

Tab. 5.4: MSS casts (one action represent a day with several (4-16) casts, total number of casts is more than 680) in the OC during MOSAiC Leg 2.

Dship Activity	Timestamp	Device	Speed (kn)	Course	Latitude (deg)	Longitude (deg)
PS122/3_30-8	2020-03-02 07:12:31	MSS_55_IOW	0,1	206,4	88,195167	31,180086
PS122/3_29-85	2020-03-01 07:53:01	MSS 46	0,1	178,6	88,22808	31,416639
PS122/3_29-76	2020-02-29 10:53:41	MSS 46	0,2	220,1	88,278203	31,954584

PS122/3_29-55	2020-02-28 11:28:38	MSS 46	0,2	225,4	88,343579	33,896732
PS122/3_29-53	2020-02-28 07:33:52	MSS 46	0,3	222,9	88,354931	34,294834
PS122/3_29-52	2020-02-28 06:15:33	MSS90L	0,2	224,4	88,358615	34,419399
PS122/3_29-42	2020-02-27 07:17:15	MSS 46	0,3	223,4	88,425294	37,289199
PS122/3_29-41	2020-02-27 07:17:05	MSS90L	0,3	223,3	88,425302	37,28951
PS122/3_29-20	2020-02-26 07:10:02	MSS 46	0,4	239,8	88,504784	40,99897
PS122/3_29-5	2020-02-25 08:10:34	MSS 46	0,5	260,7	88,567548	47,05687
PS122/3_29-1	2020-02-24 11:44:38	MSS 46	0,6	262,9	88,588778	54,502646
PS122/2_25-100	2020-02-23 07:13:46	MSS 46	0,3	290,9	88,584095	62,114512
PS122/2_25-90	2020-02-22 10:20:13	MSS 46	0,1	298,7	88,576017	64,653996
PS122/2_25-87	2020-02-22 07:54:59	MSS 46	0,1	305,4	88,573439	64,84392
PS122/2_25-77	2020-02-21 07:03:22	MSS 46	0,3	330,2	88,481177	66,890898
PS122/2_25-55	2020-02-20 06:24:34	MSS 46	0,4	315,3	88,363431	69,504511
PS122/2_25-42	2020-02-19 06:47:58	MSS 46	0,6	317,4	88,224741	74,184804
PS122/2_25-36	2020-02-18 10:23:46	MSS 46	0,4	317,6	88,105217	77,254914
PS122/2_25-6	2020-02-17 11:26:24	MSS 46	0,2	277,1	88,073456	78,889307
PS122/2_24-85	2020-02-16 10:31:54	MSS 46	0	90	88,066843	79,750912
PS122/2_24-75	2020-02-15 10:17:09	MSS 46	0	252,5	88,068882	79,816525
PS122/2_24-57	2020-02-14 10:15:05	MSS 46	0,3	312,5	88,023822	80,430635
PS122/2_24-42	2020-02-13 12:21:47	MSS 46	0,4	285,3	87,969355	83,899997
PS122/2_24-36	2020-02-12 10:37:09	MSS 46	0,4	314,8	87,874977	87,588958
PS122/2_24-22	2020-02-11 10:16:38	MSS 46	0,3	288,7	87,821849	89,979825
PS122/2_24-10	2020-02-10 10:20:54	MSS 46	0,2	314,2	87,786014	91,800664
PS122/2_23-98	2020-02-08 10:09:13	MSS 46	0,1	330,9	87,673605	93,82489
PS122/2_23-72	2020-02-07 10:18:17	MSS 46	0,1	19,6	87,640255	93,773693
PS122/2_23-71	2020-02-07 07:14:03	MSS_55_IOW	0,1	11,3	87,637174	93,75379
PS122/2_23-48	2020-02-06 06:13:18	MSS 46	0,1	346,7	87,596463	94,072935
PS122/2_23-36	2020-02-05 10:58:13	MSS 46	0,2	318,7	87,544112	94,874716
PS122/2_23-5	2020-02-03 10:37:53	MSS 46	0,2	52,8	87,419245	93,365893
PS122/2_22-96	2020-02-02 06:33:12	MSS 46	0,3	271	87,34466	95,43792
PS122/2_22-85	2020-02-01 12:51:03	MSS 46	0,3	170,4	87,388481	95,664527
PS122/2_22-72	2020-01-31 10:30:55	MSS 46	0,3	347,2	87,455533	96,385262
PS122/2_22-50	2020-01-30 06:48:50	MSS 46	0,2	121,9	87,477188	96,277744
PS122/2_22-28	2020-01-29 06:30:22	MSS 46	0,1	269	87,470651	95,222358
PS122/2_22-19	2020-01-28 10:29:32	MSS 46	0,1	315,1	87,454283	95,768973
PS122/2_22-4	2020-01-27 10:22:36	MSS 46	0,1	52,2	87,447891	95,758923
PS122/2_21-103	2020-01-24 10:36:45	MSS 46	0,1	230,3	87,421157	93,117445
PS122/2_21-113	2020-01-23 12:51:58	MSS_55_IOW	0,1	224,7	87,43904	93,911192
PS122/2_21-68	2020-01-23 06:17:23	MSS 46	0,1	227,4	87,448862	94,151709
PS122/2_21-45	2020-01-22 06:23:46	MSS 46	0,1	244,6	87,482043	95,110754
PS122/2_21-143	2020-01-21 10:00:00	MSS 46	0,2	278,1	87,488437	96,217194
PS122/2_21-19	2020-01-20 12:18:14	MSS 46	0,2	317,6	87,452237	97,370539
PS122/2_20-110	2020-01-18 11:33:21	MSS 46	0,1	185,7	87,402747	98,276781
PS122/2_20-74	2020-01-17 06:10:21	MSS 46	0,4	211,4	87,53291	99,651402
PS122/2_20-49	2020-01-16 06:20:03	MSS 46	0,2	302,5	87,553269	102,039464
PS122/2_20-27	2020-01-15 06:22:00	MSS 46	0,3	299,4	87,456024	103,736176
PS122/2_20-18	2020-01-14 11:41:06	MSS 46	0,2	308,7	87,411575	104,992222
PS122/2_20-7	2020-01-13 11:05:25	MSS 46	0,4	309,7	87,334782	107,126528

PS122/2_19-93	2020-01-11 07:17:53	MSS 46	0,3	308,2	87,212228	111,360667
PS122/2_19-83	2020-01-10 06:35:11	MSS 46	0,2	291,7	87,168098	113,096071
PS122/2_19-57	2020-01-09 06:15:22	MSS 46	0,2	299,1	87,135873	114,561307
PS122/2_19-32	2020-01-08 06:29:42	MSS 46	0	90	87,111156	115,224281
PS122/2_19-21	2020-01-07 10:32:15	MSS 46	0	114,9	87,121318	114,958088
PS122/2_19-5	2020-01-06 10:26:03	MSS 46	0,1	304,3	87,102248	115,197869
PS122/2_18-82	2020-01-04 10:58:41	MSS 46	0,2	348,2	87,003139	115,409773
PS122/2_18-59	2020-01-03 07:51:58	MSS 46	0,1	350,2	86,902153	115,737025
PS122/2_18-35	2020-01-02 06:29:49	MSS 46	0,4	321,7	86,798227	116,947392
PS122/2_18-18	2019-12-31 11:19:05	MSS 46	0,2	11,1	86,589175	117,880529
PS122/2_18-6	2019-12-30 11:36:20	MSS 46	0,3	118,1	86,597345	116,839218
PS122/2_17-88	2019-12-28 10:35:44	MSS 46	0	225,7	86,673907	115,723829
PS122/2_17-70	2019-12-27 06:13:20	MSS 46	0	333,2	86,676064	115,99658
PS122/2_17-33	2019-12-25 10:44:55	MSS 46	0,2	81,5	86,624385	114,955947
PS122/2_17-19	2019-12-24 10:30:44	MSS 46	0,1	107,1	86,624704	113,871254
PS122/2_17-9	2019-12-23 11:59:56	MSS 46	0,1	146,1	86,639982	113,164044
PS122/2_17-9	2019-12-23 11:56:14	MSS 46	0,1	143,8	86,640062	113,163056
PS122/2_17-9	2019-12-23 11:29:13	MSS 46	0,1	145,4	86,640668	113,155878
PS122/2_16-55	2019-12-21 12:47:23	MSS 46	0	208,3	86,687128	112,398353
PS122/2_16-39	2019-12-20 13:03:08	MSS 46	0,1	316,6	86,68079	112,557305
PS122/2_16-28	2019-12-19 12:41:41	MSS 46	0,1	260,8	86,678042	112,937726
PS122/2_16-47	2019-12-14 06:40:00	MSS 46	0,1	310,7	86,609519	118,552439

Tab. 5.5: VMP casts (one action represent a day with 2-3 casts) in the OC during MOSAiC Leg 2.

Dship Activity	Device	Date	aprox. Time	Longitude	Latitude
PS122/3_29-84	UIB_VMP250	2020-03-01	07:51:15	88.228127	31.416649
PS122/2_25-106	UIB_VMP250	2020-02-22	10:00:00	88.57574	64.677267

Tab. 5.6 :Fishing-rod during MOSAiC Leg 2.

Dship – action	Timestamp	Device	Latitude (deg)	Longitude (deg)
PS122/3_29-82	2020-02-29 13:20:40	CTD SST 48M_1495 fishing-rod	88,271538	31,794667
PS122/2_23-136	2020-02-06 10:00:46	CTD SST 48M_1495 fishing-rod	87,606753	94,005762
PS122/2_23-137	2020-02-06 10:00:46	CTD SST 48M_1459 fishing-rod	87,606753	94,005762
PS122/2_23-134	2020-02-06 06:10:59	CTD SST 48M_1495 fishing-rod	87,596372	94,07357
PS122/2_23-135	2020-02-06 06:10:59	CTD SST 48M_1459 fishing-rod	87,596372	94,07357
PS122/2_21-157	2020-01-23 14:22:10	CTD SST 48M_1495 fishing-rod	87,437047	93,861563
PS122/2_21-169	2020-01-23 14:10:27	CTD SST 48M_1495 fishing-rod	87,437285	93,867888
PS122/2_21-167	2020-01-23 13:40:51	CTD SST 48M_1495 fishing-rod	87,437926	93,88407
PS122/2_21-168	2020-01-23 13:16:33	CTD SST 48M_1495 fishing-rod	87,438459	93,897063
PS122/2_21-156	2020-01-23 13:11:46	CTD SST 48M_1495 fishing-rod	87,438565	93,899568
PS122/2_20-168	2020-01-19 13:02:00	CTD SST 48M_1495 fishing-rod	87,400689	98,357187
PS122/2_20-167	2020-01-19 12:53:00	CTD SST 48M_1495 fishing-rod	87,400504	98,36135
PS122/2_20-163	2020-01-18 13:34:00	CTD SST 48M_1495 fishing-rod	87,39916	98,285791
PS122/2_20-162	2020-01-18 13:34:00	CTD SST 48M_1495 fishing-rod	87,39916	98,285791
PS122/2_20-160	2020-01-18 12:45:00	CTD SST 48M_1495 fishing-rod	87,400702	98,281423
PS122/2_20-161	2020-01-18 12:45:00	CTD SST 48M_1495 fishing-rod	87,400702	98,281423

PS122/2_19-173	2020-01-12 11:59:00	CTD SST 48M_1495 fishing-rod	87,27601	109,379218
PS122/2_19-174	2020-01-11 08:26:00	CTD SST 48M_1495 fishing-rod	87,215046	111,284758
PS122/2_19-168	2020-01-08 11:31:00	CTD SST 48M_1495 fishing-rod	87,112999	115,189856
PS122/2_19-167	2020-01-08 11:20:00	CTD SST 48M_1495 fishing-rod	87,112891	115,192651

Tab. 5.7 :Fishing-rod during MOSAiC Leg 2.

Dship-action	Timestamp	Latitude (deg)	Longitude (deg)
PS122/3_29-75 LISSTDeep_4047	2020-02-29 14:08:42	88,269381	31,750532
PS122/2_25-78 LISSTDeep_4047	2020-02-21 13:59:54	88,512265	66,286071
PS122/2_23-31 LISSTDeep_4047	2020-02-05 07:44:51	87,535008	95,03844
PS122/2_22-101 LISSTDeep_4047	2020-02-02 11:16:42	87,350338	94,806241
PS122/2_22-34 LISSTDeep_4047	2020-01-29 10:44:45	87,471505	95,163075
PS122/2_21-129 LISSTDeep_4047	2020-01-26 13:09:15	87,417153	93,883285
PS122/2_21-56 LISSTDeep_4047	2020-01-22 11:30:28	87,476796	94,908424
PS122/2_20-112 LISSTDeep_4047	2020-01-19 12:02:45	87,399638	98,38041
PS122/2_20-34 LISSTDeep_4047	2020-01-15 12:37:19	87,477911	103,158638
PS122/2_19-122 LISSTDeep_4047	2020-01-12 11:30:39	87,275083	109,41506
PS122/2_19-43 LISSTDeep_4047	2020-01-08 11:01:55	87,112762	115,196805
PS122/2_18-92 LISSTDeep_4047	2020-01-05 13:25:24	87,072451	115,317462
PS122/2_18-26 LISSTDeep_4047	2020-01-01 13:27:54	86,713655	117,89103
PS122/2_16-78 LISSTDeep_4047	2019-12-22 11:31:23	86,6714	112,639966
PS122/1_11-25 LISSTDeep_4047	2019-12-11 11:36:23	86,575818	120,709984
PS122/1_10-110 LISSTDeep_4047	2019-12-08 11:50:00	86,292892	121,285791
PS122/1_10-34 LISSTDeep_4047	2019-12-04 11:20:01	86,105489	118,702339
PS122/1_10-12 LISSTDeep_4047	2019-12-01 11:27:48	85,954781	113,177389
PS122/1_9-38 LISSTDeep_4047	2019-11-27 10:48:11	86,158318	117,972393
PS122/1_8-17 LISSTDeep_4047	2019-11-19 11:10:15	85,793615	120,753999
PS122/1_7-42 LISSTDeep_4047	2019-11-13 09:55:04	86,110892	117,973391
PS122/1_6-123 LISSTDeep_4047	2019-11-10 09:25:08	85,823635	116,111647
PS122/1_6-145 LISSTDeep_4047	2019-11-05 06:23:49	85,948338	118,751798